

Berkeley, December 23<sup>rd</sup> 2015

Dear Dr. Archfield and Reviewers,

Thank you very much for the helpful feedback on the manuscript and for the opportunity to submit a revised version. All changes are indicated in blue in the marked up manuscript and supplementary materials below.

In revising the manuscript, we have closely followed the changes proposed in the point-by-point responses to the reviewers' comments that were made during the open discussion. We have therefore not duplicated these responses here, but simply summarize the main changes made:

1. We clarified the two key conceptual points brought up by the reviewers, namely:
  - a. Errors on the process-based model are driven by parameter estimation uncertainties (l 445-459). However, we purposely chose to not disentangle them from errors on the modeled processes themselves because (i) process-related errors were already assessed in a previous paper (Muller 2014 WRR) and (ii) we'd like to assess operational modeling performances in ungauged basins, where these error sources are confounded (l 156-161).
  - b. While more complex (and presumably more accurate) statistical methods exist, Chalise 2003 is the most adapted (in terms of data requirements) recent statistical approach for the considered region. It is also the most likely statistical approach to be used for practical purposes in Nepal. (l. 190-198).
2. A descriptive flow chart (Figure 2) was added to clarify the numerical method used to assess prediction performances under change.
3. We added minimum and maximum values to the catchments characteristics presented in Table 1.
4. The discussion on the attribution of sources of uncertainty (Section 4.1.1) is considerably shortened. It now only presents the main results drawn from the additional cross-validation analyses, now presented in supplementary materials.
5. The discussion relating catchment characteristics to the performance of the statistical method for prediction under change (Section 4.2) is considerably shortened as well. The discussion on the resilience of flow regimes and the related Monte Carlo analysis are now presented in supplementary materials.

We hope that these changes address the reviewers' concerns and improve the legibility of the manuscript. Thank you again for your consideration.

Yours truly,

Marc Muller and Sally Thompson

# Comparing statistical and process-based flow duration curve models in ungauged basins and changing rain regimes

Marc F. Müller<sup>1</sup> and Sally E. Thompson<sup>1</sup>

<sup>1</sup>Department of Civil and Environmental Engineering, Davis Hall, University of California, Berkeley CA, USA

*Correspondence to:* Marc F. Müller (marc.f.muller@gmail.com)

**Abstract.** The prediction of flow duration curves (FDCs) in ungauged basins remains an important task for hydrologists given the practical relevance of FDCs for water management and infrastructure design. Predicting FDCs in ungauged basins typically requires spatial interpolation of statistical or model parameters. This task is complicated if climate becomes non-stationary, as the prediction challenge now also requires extrapolation through time. In this context, process-based models for FDCs that mechanistically link the streamflow distribution to climate and landscape factors may have an advantage over purely statistical methods to predict FDCs.

This study compares a stochastic (process-based) and statistical method for FDC prediction in both stationary and non-stationary contexts, using Nepal as a case study. Under contemporary conditions, both models perform well in predicting FDCs, with Nash-Sutcliffe coefficients above 0.80 in 75% of the tested catchments. The main drivers of uncertainty differ between the models: parameter interpolation was the main source of error for the statistical model, while violations of the assumptions of the process-based model represented the main source of its error. The process-based approach performed better than the statistical approach in numerical simulations with non-stationary climate drivers. The predictions of the statistical method under non-stationary rainfall conditions were poor if (i) local runoff coefficients were not accurately determined from the gauge network, or (ii) streamflow variability was strongly affected by changes in rainfall. A Monte Carlo analysis shows that the streamflow regimes in catchments characterized by frequent wet-season runoff and a rapid, strongly non-linear hydrologic response are particularly sensitive to changes in rainfall statistics. In these cases, process-based prediction approaches are favored over statistical models.

## 1 Introduction

The flow duration curve (FDC) provides a compact summary of the variability of daily streamflow by indicating what proportion of the flow regime exceeds a given flow rate. FDCs have considerable practical relevance, particularly in supporting decisions that are affected by the availability and reliability of surface water. Common applications of FDCs include the design and management of hydropower infrastructure (e.g., Basso and Botter, 2012; Müller, 2015), the determination of environmental flow standards for ecosystem protection (e.g., Lazzaro et al., 2013), the allocation of water resources for consumptive uses (e.g., Alaouze, 1989) [or the prediction of streamflow time series in ungauged or poorly gauged catchments \(e.g., Hughes and Smakhtin, 1996; Westerberg et al., 2014\).](#)

Despite their utility, empirical FDCs are unavailable for many basins, primarily because they require extensive on-site observations of daily streamflow (Vogel and Fennessey, 1994). Globally, the majority of catchments remain ungauged (or the gauge data that exist are subject to significant quality assurance and data availability constraints). Furthermore, the global number of stream gauges continues to decline because of ongoing budgetary constraints faced by water monitoring agencies (Stokstad, 1999; United States Geological Survey, 2015). Therefore FDCs must typically be estimated in data-scarce areas. The most widely used techniques for FDC estimation are simple, graphical methods. Such empirical methods are easy to implement but often rely on overly simplistic assumptions that lead to substantial prediction errors. For instance in Nepal, the regionalization method prescribed in official design manuals (e.g., Chitrakar, 2004; Alternative Energy Promotion Center, 2014) relies on *one* in-situ observation of streamflow during the dry season to scale standardized regional indices for monthly flows. The procedure neglects the inter-annual variability of low-flows, which leads to important biases in the predicted flow distributions ([see Section S1 of Supplementary Materials](#)). Even in gauged catchments, FDCs constructed from historical observations may not represent current flow conditions well, because flow regimes are impacted by climate change and anthropogenic alterations of the catchments (e.g. Botter et al., 2013; Mu et al., 2007). Predicting streamflow in ungauged basins, particularly in the context of environmental change, remains both a fundamental necessity for water managers and a major research challenge (Blöschl et al., 2013; Montanari et al., 2013).

Recent efforts to predict FDCs in ungauged catchments focus on statistical approaches that predict the flow distribution based on the catchment's similarity to nearby, gauged watersheds (Castellarin et al., 2013). Index flow approaches, which regionalize specific index flows (typically the mean flow), and use those indices to rescale empirical FDCs from similar catchments, are particularly popular (e.g., Chalise et al., 2003; Castellarin et al., 2004b; Sauquet and Catalogne, 2011; Arora et al., 2005). While differing in methodological details, all index flow approaches assume that FDCs do not vary within homogeneous regions, except by a scaling factor. Because they do not assume any specific runoff-generating process, statistical methods are versatile. They have been successfully

been applied globally to predict FDCs in a variety of climates and catchment types (Blöschl et al., 2013). However, methods are also insensitive to the diversity of controls on the shape of the FDC  
60 exerted by climate processes and catchment characteristics. This may affect their reliability under non-stationary conditions (Milly et al., 2008). Finally, the calibration of statistical methods relies on extensive streamflow observations from a large number of representative and well characterized catchments (e.g., Cheng et al., 2012; Coopersmith et al., 2012). Their performance is therefore sensitive to the spatial density of available gauges Blöschl et al. (2013), and their reliability in regions  
65 where streamflow data is truly scarce is uncertain.

Stochastic, process-based models that mechanistically link the drivers, state and response of the system are a promising avenue to address these issues. In these models, basic assumptions about the stochastic structure of rainfall and the (deterministic) response of catchments allow the analytic derivation of streamflow probability density functions (PDFs). (Note that because the FDC can be  
70 obtained directly by transforming the PDF, a predictive technique that yields the streamflow PDF will also allow the FDC to be estimated). Botter et al. (2007b) show that runoff follows a gamma distribution if catchments behave as a linear reservoir, forced by stochastic rainfall that follows a marked Poisson process. The resulting gamma distribution depends on two parameters that are determined by the recession characteristics of the catchment, and by the frequency and intensity of  
75 effective rain. This process-based approach to the streamflow PDF has been extended to include the fast flow component of streamflow (Muneepeerakul et al., 2010), non-linearities in subsurface storage-runoff relationships (Botter et al., 2009), the effects of short-term snowmelt (Schaeffli et al., 2013) and the carryover of subsurface storage between seasons in seasonally dry climates (Müller et al., 2014). Although the stochastic framework allows the effects of changes in climate or land-  
80 scape to be independently modeled, it relies on strong simplifying assumptions about the spatial homogeneity of catchments. These assumptions makes the existing process models less versatile than statistical methods. Nonetheless, the approach has low calibration requirements because it relies on a small number of parameters, which can be determined using rainfall, climate and geomorphological characteristics of the catchments (Doulatyari et al., 2015). This information is increasingly available  
85 in ungauged basins, thanks to remote-sensing technologies, even when ground-based measurements are sparse.

Process-based models successfully reproduce streamflow PDFs in numerous [gauged](#) catchments worldwide (Botter et al., 2007a; Ceola et al., 2010), [including Nepal \(Müller et al., 2014\)](#). Yet their [predictive performance in ungauged basins remains largely unassessed, particularly in regions where](#)  
90 [the local gauge density is globally representative \(as opposed to densely monitored catchments in developed countries such as, e.g., France and Austria in Castellarin et al. \(2013\)\)](#). For lower gauge densities, it is unclear whether the advantages of the process-based approaches, which are derived from an explicit representation of flow-generating processes, are outweighed by the limitations im-

posed by the restrictive assumptions underlying these methods - and whether this trade-off is altered

95 by non-stationarity in climate drivers.

Using Nepal as a test case, this study compares the process-based and statistical approaches on the basis of (i) their ability to predict FDCs in ungauged basins, (ii) their sensitivity to data-scarcity, represented both by the spatial density of the stream gauge network and by the temporal extent (length) of the available streamflow records, and (iii) their ability to accommodate changes in the

100 rainfall regime.

Nepal provides an ideal setting to compare the two approaches, for four reasons. First, the country is representative of global availability of streamflow data, as measured by the density of its stream gauge network (Figure 1(a)). Second, methods drawn from both statistical and process-based approaches have been developed and validated in Nepal. Here we compare the stochastic-dynamic  
105 framework developed in Müller et al. (2014), with the index flow model described in Chalise et al. (2003). Third, flow generation processes in Nepalese Himalayan catchments are complex, particularly with respect to the spatial and temporal properties of precipitation. Rainfall derives from the Indian Summer Monsoon and is strongly affected by topography. As a result, local rainfall is temporally autocorrelated, spatially heterogeneous and highly seasonal. There is also significant carryover  
110 of groundwater storage between the wet and dry seasons, so that dry season discharge reflects the features of the antecedent wet season. These characteristics violate many of the assumptions that underlie the process-based method. The analysis in Nepal is therefore likely to provide a conservative estimate of the potential performance of the process-based method in ungauged basins. Finally, developing reliable methods for FDC prediction in Nepal represents an opportunity for ‘use-inspired  
115 science’ (Thompson et al., 2013b). Nepal has an enormous untapped hydropower potential and is in dire need of electrical power, particularly in rural areas. A reliable method to estimate FDCs in ungauged catchments would be a valuable tool to support the development of micro hydropower, a sustainable technology for rural electrification (Müller, 2015).

Section 2 describes the two models and the procedures used to estimate their parameters from  
120 streamflow and rainfall observations. Section 3 presents the results of the comparative analysis in Nepal. Section 4 examines the key sources of errors for both models and discusses implications for both Prediction in Ungauged Catchments (PUB) and Predictions Under Change (PUC) beyond Nepal.

## 2 Methods

### 2.1 Compared Approaches

#### 2.1.1 Process-based model

The process-based approach models daily streamflow as a random variable. Subject to strong simplifying assumptions about rainfall stochasticity and runoff generation, the streamflow PDF can be analytically derived. During the wet season, daily rainfall is represented as a stationary marked Poisson process with exponentially distributed depths. Assuming linear evapotranspiration losses, Botter et al. (2007b) showed that effective rain, that is the portion of the total rainfall that contributes to streamflow generation, also follows a stationary marked Poisson process. For a spatially homogeneous catchments with an exponentially distributed response time (i.e. a catchment that behaves as a linear reservoir), this effective rainfall will produce gamma-distributed streamflow. The parameters of the gamma distribution are derived from the frequency ( $\lambda_P$ ) and mean depth ( $\alpha_P$ ) of rainfall, and from the recession constant ( $k$ ) of the catchment. If rainfall in the dry season is sufficiently minimal that effective rainfall does not contribute to runoff generation, then dry season streamflow represents only the discharge of groundwater stored during the previous wet season. This discharge is modeled as a single seasonal recession with stochastic initial conditions that depend on the wet season properties. Because groundwater is not replenished during the dry season, the water table is subject to a large transient drawdown, resulting in a nonlinear discharge behavior and a power law relation between recession rate and discharge (Brutsaert and Nieber, 1977). We showed in Müller et al. (2014) that the distribution of streamflow, and therefore the FDC, in seasonally dry climates that meet the assumptions above can be expressed analytically as a function of seven independent parameters: the frequency ( $\lambda_P$ ) and mean intensity ( $\alpha_P$ ) of wet season rainfall, maximum daily evapotranspiration during the wet season ( $ET$ ), the water storage capacity of the soil in the root zone ( $SSC$ ), the (linear) wet-season recession constant ( $k$ ), the duration of the dry season ( $T_d$ ) and the exponent of the power law recession during the dry season ( $b$ ). The model admits an additional input parameters, the scale  $a$  of the of the power-law seasonal recession, which we showed in Müller et al. (2014) can be expressed as a function of  $k$ ,  $b$ ,  $\lambda_P$  and  $\alpha_P$ . The formal derivation of the model is summarized in Appendix A.

The model was successfully validated in a variety of regions with seasonally dry climates worldwide, including Nepal, where observed FDCs were predicted in 24 gauged catchments with a median Nash Sutcliffe Coefficient of 0.90 on log-transformed flow quantiles (Müller et al., 2014). The approach successfully reproduced both the rain-driven distribution of flows during the wet season and the release of stored monsoon water during the dry season recession. In this study, we assess the operational performance of the process-based approach as a tool to predict streamflow in *ungauged* catchments. Therefore, we do not further attempt to attribute model errors to parameters versus the

model structure in the results presented in Section 3, since in practice these errors are confounded in any real application. The relative significance of these two error sources is nonetheless discussed in Section 4.1.1.

In ungauged catchments, the process-based model is implemented as follows. Three of the seven parameters of the model ( $T_d$ ,  $\lambda_P$ ,  $\alpha_P$ ) are rainfall characteristics that can be estimated in ungauged basins using meteorological observations. Recession parameters ( $k$  and  $b$ ) describe aquifer properties that are challenging to observe at the catchment scale. They can be estimated using observed streamflow time series in nearby gauged basins, and subsequently interpolated from nearby gauges, using the geostatistical approach described in Müller and Thompson (2015), which accounts for the topology of the stream network. The last two parameters ( $ET$ ) and ( $SSC$ ) describe catchment-scale soil moisture dynamics that are arduous to determine empirically. Previous applications of the model relied on reasonable values of  $ET$  and  $SSC$ , based on land use, soil and climate characteristics of the catchment (e.g., Botter et al., 2007a; Ceola et al., 2010). Alternatively, runoff coefficients can be used to directly relate rainfall statistics to streamflow increments (Doulatyari et al., 2015). Runoff coefficients describe the ratio of mean discharge to mean precipitation, and can be predicted in ungauged basins using water balance models and meteorological observations. This approach circumvents the need to estimate  $ET$  and  $SSC$ , but the accuracy of predicted runoff coefficients in ungauged catchment is critically dependent on the type of water balance model used and on the availability of appropriate calibration data (Doulatyari et al., 2015). Instead, this study follows the former procedure and uses reasonable estimates of  $ET$  and  $SSC$  for Nepal.

### 2.1.2 Statistical model

The statistical approach is entirely driven by observation data and does not assume any specific runoff generation process. Instead, it identifies and exploits statistical correlations that may occur between streamflow observed at existing gauges and the geology, topography and climate of the corresponding catchments. The index flow model used in this study was developed by Chalise et al. (2003) to regionalize FDCs in Nepal to assess the potential for small hydropower development. The model is based on local flow indices for mean ( $Q_m = E[Q]$ ) and low flows ( $q_{95} = Q_{95}/Q_m$ , where  $Q_{95}$  is the 95<sup>th</sup> streamflow percentile) and uses a non-parametric approach to represent the shape of the FDC. Empirical FDCs from available gauges are normalized by  $Q_m$  and pooled into equally-sized groups based on the  $q_{95}$  index of the gauge. A standardized curve is determined for each group by taking the average of the normalized flows corresponding to each duration, in order to represent the average catchment response in the group. The chosen statistical approach is considerably less complex than many alternative state-of-the-art methods using multiple (often non-linear) equations to relate multiple flow quantiles to a variety of observed covariates (see Castellarin et al. (2013) for a review). However, Chalise et al. (2003) is, to our knowledge, the most recent statistical method specifically developed and validated in the study region. The approach is parsimonious and adapted

to situations, where in-situ observations of catchment characteristics are scarce. The method is therefore representative of the level of complexity of statistical approaches likely to be implemented in developing countries practical hydrological engineering purposes.

Predictions in ungauged catchments are obtained by first using linear regressions to predict  $Q_m$  and  $q_{95}$ . Although the original method calls for a stepwise multiple regressions approach to determine regression covariates inductively, we used the regression models obtained in Chalise et al. (2003):  $Q_m$  is regressed against annual rainfall ( $R_y$ ) and gauge elevation ( $z_{min}$ ) as a proxy for evapotranspiration; and  $q_{95}$  is regressed against the ratios of catchment area occupied by each of the considered geological units. The two regressions loosely represent the long term water balance and short-term response of the catchment. The predicted low-flow index is then used to determine the standardized FDC shape, which is finally multiplied by the predicted mean flow to obtain the FDC. An important assumption, inherent to the linear regression models, is that the dependent variable (here  $Q_m$  and  $q_{95}$ ) is not spatially correlated, when controlling for the considered covariates. This assumption is reasonable in Nepal, where the typical distance between stream gauges is much larger than the correlation scale of runoff (Müller and Thompson, 2015). In more densely gauged areas (or if runoff is correlated over larger distances), streamflow observations at neighboring or flow-connected gauges are likely to be correlated. In these regions, accounting for the effect of distance and stream network topology when interpolating flow indices (e.g., using TopREML (Müller and Thompson, 2015)) will improve predictions.

## 2.2 Study region and data

The two methods were evaluated using observed streamflow data from 25 Nepalese catchments mapped in Figure 1 (b). The gauges in this dataset (HKH-FRIEND, 2004; Department of Hydrology and Meteorology, 2011) have at least 10 years of daily streamflow records. They were checked for consistency, using double mass plots (Searcy and Hardison, 1960), and bias: we discarded non-glaciated catchments that had a precipitation deficit on their long term water balance. Watersheds were delineated using the ASTER GDEM v2 digital elevation model (NASA Land Processes Distributed Active Archive Center (LP DAAC), 2011). The study watersheds are located in central Nepal but cover a wide variety of catchment sizes, elevation ranges, precipitation characteristics and geological units (Table 1).

We focused on the Chepe Kohla catchment in central Nepal (Figure 1 (b, insert)) as a case study for analyses requiring resampling (Section 2.3.1) or simulation (Section 2.3.2) of streamflow time series. The Chepe Kohla watershed has a long (by Nepalese standards) record of daily streamflow observations (31 years) and is representative of the full sample of gauges in terms of topography and recession behavior (Table 1). The catchment is also small (i.e. close to spatially homogenous) and local rainfall is well approximated by a marked Poisson process (First order autocorrelation



230 coefficient of rainfall occurrence (AR): 0.09, Coefficient of variation of rainfall depths (CV): 1.09),  
echoing the underlying assumptions of the process-based model.

Rainfall characteristics over the sampled catchments were obtained from 178 precipitation gauges (HKH-FRIEND, 2004; Department of Hydrology and Meteorology, 2011), also mapped on Figure 1 (b). The average duration of the dry season ( $T_d$ ) was estimated at each precipitation gauge by fitting a step function to the corresponding rainfall time series (Müller and Thompson, 2013), and wet-season precipitation records were used to compute the frequency and mean intensity of rainfall ( $\lambda_P$  and  $\alpha_P$ ). Rainfall characteristics were then aggregated at the catchment level by assuming that the rain process aggregates linearly within the basins. For rainfall occurrence, we assumed that the duration between rain events caused by two consecutive storms can be estimated as the average of the inter-arrival times measured at the rain gauges within the catchment. This allows us to compute catchment level rainfall frequency as:

$$\lambda_P = \left( \frac{1}{N_g} \sum_i^{N_g} \frac{1}{\lambda_P^{(i)}} \right)^{-1}$$

where  $\lambda_P^{(i)}$  designates rainfall frequency observed at gauge  $i$  and  $N_g$  the number of rain gauges within the catchment. Similarly, the catchment-level duration between rainy seasons is assumed to be the average of the durations observed within the catchment:

$$T_d = \frac{1}{N_g} \sum_i^{N_g} T_d^{(i)}$$

Finally, the precipitation depth received on any given day by a catchment is assumed to be the average of the precipitation depths observed by individual rain gauges. It follows that the aggregated mean rainfall intensity can be expressed as:

$$\alpha_P = \lambda_P^{-1} \frac{1}{N_g} \sum_i^{N_g} \lambda_P^{(i)} \alpha_P^{(i)}$$

If no precipitation station is located within the catchment, rainfall characteristics observed at the rain station closest to the catchment centroid were considered. *Although aggregating rainfall time series before computing their statistics would better account for spatial correlation in rainfall, aggregating rainfall statistics instead allows for non-overlapping observation periods (assuming rainfall is stationary). This is important in the context of Nepal, where rain gauges are scarce with sporadic observations. Unfortunately, the low density of rain gauges within the considered basins prevents a formal treatment of spatial correlation when aggregating frequencies. However, in a previous study (Müller and Thompson, 2013) we observed large spatial correlation ranges on rainfall occurrence in Nepal (125km during the monsoon). Under these conditions the selected method stands out as the most parsimonious approach to utilize multiple, yet sparse, rainfall observations.*

235  
240

Recession characteristics were estimated using streamflow observations as described in Müller et al. (2014). We computed wet season recession constants ( $k$ ) by regressing the logarithm of stream-

flow against time for each period of consecutively decreasing streamflow during the wet season. The  
 245 recession constant was then obtained by taking the median value of the regression coefficients of  
 recessions lasting more than four days. The power law exponent of dry season recessions ( $b$ ) was  
 obtained by fitting a non-linear recession curve

$$Q(t) = (Q_0^{1-b} - a(1-b)t)^{\frac{1}{1-b}} \quad (1)$$

to base flow, which was computed from observed streamflow time series using the Lyne Hollick  
 250 algorithm (Nathan and McMahon, 1990). The last streamflow peak of the wet season was taken as  
 initial flow condition  $Q_0$ , and we used a stochastic optimization algorithm (Simulated Annealing,  
 Bélisle (1992)) to minimize least square fitting errors. In ungauged catchments, the scale exponent  
 of the seasonal recession was approximated as (Müller et al., 2014):

$$a \approx \frac{\lambda}{-r} \left( e^{\frac{-r}{m}} - 1 \right) (\alpha_Q \cdot (m+1)), \quad (2)$$

255 where  $r = 1 - b$ ;  $m$  is the ratio between the frequency  $\lambda$  of effective rain events and the linear  
 recession constant  $k$ , and  $\alpha_Q$  is the average depth of effective rain events (see Appendix A).

Potential evapotranspiration was approximated by applying the empirical relation estimated by  
 Lambert and Chitrakar (1989) for Nepal during the rainy season (July-September):

$$ET \approx 4.0 - 0.0008 \cdot z_{mean}$$

where  $ET$  is given in  $[mm/d]$  and  $z_{mean}$  is the average elevation of the catchment in meters. The  
 formula provides daily average evapotranspiration estimates for each month. It accounts for elevation  
 but assumes a spatially homogenous elevation gradient. A uniform soil moisture capacity of 50  
 260 mm was assumed throughout the country, based on empirical observations reported in Shrestha  
 (1997). By neglecting local variation in soil characteristics, this produces conservative estimates  
 of the performance of the process-based model in ungauged basins.

## 2.3 Comparative Analyses

### 2.3.1 Predictions in Ungauged Basins

265 We used three cross-validation techniques to evaluate the predictive ability of both methods in un-  
 gauged basins. Firstly, a leave-one-out analysis was carried out to assess predictive performances  
 in a realistic situation, where FDCs are predicted in Nepal using all streamflow gauges available in  
 the region. Secondly, we examined the sensitivity of the methods to decreasing data-availability by  
 reducing the number of gauges available to calibrate the models. Finally, we performed a similar  
 270 data-degradation procedure, but in this case we reduced the number of daily streamflow observa-  
 tions, while holding the number of gauges constant. This final analysis accounts for the challenges  
 posed by recent or temporary installation of stream gauges, which introduce uncertainties into the

estimation of model parameters due to the short streamflow records used. These errors can propagate through the model and affect the prediction of FDCs.

In a leave-one-out analysis, one gauge is ‘left out’ of the dataset, and streamflow is predicted at the ‘missing’ location using observations from the remaining gauges. The predicted FDC is then compared to observations from the omitted gauge. The resulting error between observation and prediction yields the prediction performance of the method at that catchment if it were not gauged. Repeating the procedure for all gauges offers an approximation to the overall prediction error of the method. To measure this error we constructed error duration curves (Müller et al., 2014), where the relative prediction error at each flow quantile is plotted against the corresponding duration. Error duration curves allow the partitioning of prediction errors across flow quantiles to be visualized. General prediction performances (across all durations) at individual gauges were also determined using the Nash Sutcliffe coefficient (NSC) on log streamflow quantiles (Müller et al., 2014):

$$NSC = 1 - \frac{\sum_{t=1}^{364} \left( \ln Q_t^{(emp)} - \ln Q_t^{(mod)} \right)^2}{\sum_{t=1}^{364} \left( \ln Q_t^{(emp)} - E \left[ \ln Q_t^{(emp)} \right] \right)^2} \quad (3)$$

where  $Q_t^{(emp)}$  and  $Q_t^{(mod)}$  are the empirical and modeled streamflow quantile of duration  $t$ .

The effect of the number of calibration gauges was assessed using a Jack-Knife cross-validation analysis (Shao and Tu, 2012; Müller and Thompson, 2013). At each of 10,000 iterations, a selected fraction of the available gauges was randomly sampled (without replacement) and used to predict the FDC at one (randomly selected) remaining gauge. Prediction accuracies for flow duration curves (given by the  $NSC$ ) and uncertainties on the spatial interpolation of model parameters were reported for each iteration. The procedure was repeated for decreasing numbers of selected ‘training’ gauges.

The available streamflow data did not allow a direct evaluation of the effects of timeseries length through cross-validation, because such an analysis requires substantial overlaps in the monitoring periods of all gauges. Therefore we focused the final analysis on the Chepe Kohla catchment which has the longest observation record in our dataset. We evaluated the effect of the length of the available observation records on parameter estimation, and propagated the ensuing uncertainty in the parameters to the FDCs predicted by each model. To do this, we selected a fixed number of full years of streamflow observations, estimated the parameters, predicted the FDC using these parameters, and compared the results to the empirical FDC obtained from the full observation record. The procedure was repeated 10,000 times. The estimation errors in the model parameters and the resulting FDC prediction performances ( $NSC$ ) were recorded as a function of the number of sampled years. This analysis is not intended to describe the models’ ability to predict FDCs at catchments with short observation records: in this case, constructing an empirical FDC using the available (however short) observation record is likely to be the best course of action (Castellari et al., 2004a). Instead, the analysis is intended to simulate the effect of short observation records on FDC prediction at nearby, *ungauged* catchments. The underlying assumptions behind this analysis are that (i) the error associ-

ated with interpolation is independent of the flow record length, and (ii) the Chepe Kohla catchment is representative of Nepalese basins .

### 310 2.3.2 Predictions Under Change

We used numerical simulations to assess the ability of both models to predict streamflow when subject to changing rainfall regimes, as described in Figure 2.

Synthetic streamflow time series were generated by coupling the stochastic rainfall generator described in Müller and Thompson (2013) to a rainfall-runoff model. The generated wet-season rainfall  
315 is a first order Markov process (i.e. rainfall occurrence on a given day is correlated to rainfall occurrence on the previous day) with gamma-distributed rainfall intensities, and as such produces a rainfall record that explicitly violates the assumptions under-pinning the process-based model. The duration of the rainy season was assumed constant, and no rainfall was generated during the dry season. Wet-season streamflow was simulated by feeding synthetic rainfall into a linear reservoir (with a  
320 recession constant  $k$ ) with linear evapotranspiration losses, as in Müller et al. (2014). Dry season discharge was obtained by simulating non-linear seasonal recessions of duration  $T_d$  starting at randomly selected runoff peaks in the (previously generated) wet-season streamflow. These assumptions are close to the observed reality in Nepal, as seen in Figure 5 (a), where the FDC constructed from the simulated streamflow is a close approximation to the empirical FDC in the Chepe Kohla watershed.  
325 We translated the effect of shifts in precipitation regimes into changed streamflow for the Chepe Kohla catchment by considering a range of future combinations for rainfall frequencies and intensities. In line with what is expected in Nepal (Turner and Slingo, 2009; Turner and Annamalai, 2012), we considered negative changes in the frequency and positive changes in the mean daily rainfall depth. We neglected changes in soil moisture capacity, evapotranspiration, rainfall autocorrelation  
330 and the duration of the rainy season. These parameters are explicit in the process-based model, so we expect differences in the sensitivity of the process-based and statistical models to climate change to be underestimated by this procedure. For each rainfall scenario, we evaluated the performance of the models in a changing climate by generating 1000 years of daily streamflow using future rainfall frequencies and intensities.

335 We compared the synthetic FDCs to model predictions that were made with *future* rainfall statistics, but *contemporary* recession and low flow parameters (Figure 2). The statistical method in Chalise et al. (2003) uses a linear regression over a cross-sectional sample of observations to predict mean flow based on mean rainfall and altitude. The regression may fail to capture a variety of unobserved characteristics affecting both rainfall and streamflow (e.g., local topographic features),  
340 and hence may not capture the causal relation between the two variables. The extent of this bias cannot be quantified a priori, so we considered two extreme cases: infinite and zero bias. The infinite bias case (Case 1 on Figure 2) represents the case where no effective relationship can be determined between rainfall and mean flow. The best estimator of future mean flow is then the *current* flow

condition. Conversely, if regression coefficients perfectly describe the effect of annual rainfall on average flow (Case 2 on Figure 2), then the future flow conditions can be perfectly estimated using the (known) future annual rainfall. We modeled this situation by estimating  $Q_m$  directly from the (simulated) *future* flow conditions. While the two cases differed in the determination of mean flow ( $Q_m$ ), the low-flow parameter ( $q_{95}$ ) was determined from current flow conditions in both cases. In Chalise et al. (2003),  $q_{95}$  is normalized by  $Q_m$  and represents recession behavior, which is assumed independent from rainfall. The process-based predictions were obtained by inserting future rainfall statistics and contemporary recession constants into the analytical FDC equation described in Appendix A. The two models were compared by plotting prediction performances ( $NSC$ ) against the relative change in the frequency and intensity of synthetic rainfall.

Although the recession assumptions of the process-based model are taken to generate the synthetic streamflow used as control, we believe that the analysis is not biased against the statistical approach for three reasons. Firstly, the only parameter of the statistical approach that is influenced by rainfall ( $Q_m$ ) is also computed from synthetic streamflow (Case 2 on Figure 2). Secondly, although based on identical recession assumptions, the process-based model and the synthetic streamflow generator are driven by different stochastic rainfall processes (i.e. Poisson and Markov respectively). Lastly and most importantly, empirical observations reveal that synthetic streamflow distributions generated under contemporaneous rainfall conditions reproduce closely FDCs constructed from gauge records (Figure 5 (a)), showing that the underlying recession assumptions are, in fact, representative with runoff processes actually occurring in Nepal.

### 3 Results

#### 3.1 Prediction in Ungauged Basins

Results from the leave-one-out cross-validation analysis are presented in Figure 3 and show that both methods perform similarly in the prediction of FDCs in ungauged basins. Error duration curves (Figure 3 (a) and (b)) show comparable streamflow prediction uncertainties: 75% of the predicted flow quantiles are between half and double the observed streamflow for both models, although the low flows in the process-based model display an increasing upwards bias (Figure 3 (b)). Considering the Nash-Sutcliffe coefficients computed at the individual basin level, the mean and median performances are again comparable for both models, but the accuracy of the statistical model predictions are more variable across sites than the process model predictions, as indicated by the larger spread of the Nash Sutcliffe coefficients (Figure 3(c)).

Figure 4 (a, top) shows prediction performances of both models as the number of streamflow gauges available for predictions decreases, and indicates that the performance of both models is relatively insensitive to the gauge density, until it declines to less than approximately 0.6 gauges per 10,000 km<sup>2</sup>. For such situations, which represent discarding more than half the available gauges

in Nepal, the statistical model performance declines rapidly compared to the process-based model.

380 Prediction performances are strongly affected by uncertainties on the interpolation of model parameters, as seen in Figure 4 (a, bottom). Interpolation uncertainties are generally larger for the flow indices of the statistical model ( $Q_m$  and  $q_{95}$ ) than for the recession parameters of the process-based model ( $k$  and  $b$ ). This explains the larger spread in prediction performances of the former (Figure 3 (c) and error bars in Figure 4 (a, top)). The parameter uncertainties are also relatively insensitive  
385 to the total gauge density until about 60% of the originally available gauges are discarded. At this point, the uncertainties associated with estimation of the flow indices increase significantly, while the process-based model parameters remain more reasonably estimated.

When considering short observation windows, parameter uncertainties also drive the performance of the models. Figure 4 (b, top) shows the prediction performance of both models at the Chepe Khola  
390 watershed, as the number of observation years used to estimate the model parameters is reduced. In this case, the statistical model outperforms the process-based model when less than 10 years of streamflow observations are available. The parameter uncertainties associated with the short time-series estimates (Figure 4 (b, bottom)) suggest that a longer time series of streamflow observations is needed to accurately estimate the wet-season recession parameter ( $k$ ), resulting in the lower per-  
395 formance of the process-based model for short streamflow records.

### 3.2 Prediction Under Change

Simulation results presented in Figure 5 (b) show both models' ability to predict a simulated future flow duration curve of the Chepe Kohla River, under a range of different possible changes in rainfall regimes. In all simulations, parameters describing the hydrological response of the basin ( $k$ ,  $b$ ,  
400 and  $q_{95}$ ) are determined using current flow conditions, and evapotranspiration is assumed constant. The results show that explicitly modeling rainfall-runoff processes allows the process-based model to accommodate the effects of the changing precipitation regime. In contrast, the performance of the statistical model is affected at various degrees by shifts in rainfall regimes, depending on how the model translates changes in annual precipitation to changes in average flows. If these shifts are  
405 perfectly represented by the model, then prediction errors arise solely from changes in the shape of the FDC, and the process and statistical models perform similarly in the Chepe Kohla watershed across the full range of considered rainfall scenarios (Figure 5 (b), dashed curve). If, however, average (future) streamflows cannot be reliably predicted from the predicted changes in annual rainfall, the statistical model does not accommodate flow regime changes at all. In this case, future FDCs are  
410 modeled using current streamflow observations, and the ensuing prediction errors can be substantial (Figure 5 (b), dotted curve). The simulated cases provide upper and lower bounds for the actual performance of the statistical model in future rainfall regimes. We evaluated the model's ability to predict  $Q_m$  by using cross sectional data (i.e. average streamflow and annual rainfall from the 25 catchments) to estimate the linear relation between  $Q_m$  and annual rainfall  $R_y$ . Applied to the Chepe

Kohla watershed, the estimated regression coefficients allowed the annual streamflow to be estimated from annual precipitation with a bias of  $-13\%$  and a coefficient of determination of  $R^2 = 0.57$  (Figure 5 (c)). Regardless, prediction errors remained negligible for both bounds ( $NSC > 0.95$ ) for the range of changes actually anticipated in Nepal (e.g.,  $\Delta\lambda_P/\lambda_P \approx 0.98$  and  $\Delta\alpha_P/\alpha_P \approx 1.20$  for the  $2 \cdot CO_2$  scenario (Turner and Slingo, 2009)).

## 4 Discussion

### 4.1 Predictions in Ungauged Basins

The analysis suggests that both statistical and process-based methods to estimate FDCs in ungauged basins perform comparably in Nepal, over a wide range of gauge densities and observation durations. Yet prediction performances varied significantly between the models as data became increasingly sparse. The statistical method is more sensitive to spatially sparse data, which degrades the interpolation accuracy of  $Q_m$ . In contrast, the estimation method for recession parameters makes the process-based approach more sensitive to temporally restricted observations, which reduce the accuracy with which recession parameters can be estimated. This suggests that the performance of the two models in ungauged basins is affected by different sources of uncertainty. In this section, we investigate the source of prediction error in each methods and discuss the implications for their application in ungauged basins beyond Nepal.

#### 4.1.1 Sources of Uncertainty

The statistical model relies on two assumptions about the correlations of observed data. The first assumption is that catchments with similar low-flow indices ( $q_{95}$ ) have identical hydrological responses, and therefore identical FDC shapes. Second, the model assumes that the flow indices ( $Q_m$  and  $q_{95}$ ) at ungauged catchments can be best predicted using linear regressions against observable covariates (annual rainfall, elevation and geology). The latter assumption does not hold if the flow indices are spatially auto-correlated, or if the posited linear relations are spatially heterogeneous or, in fact, non-linear. Further, ‘omitted variable’ biases (Greene, 2003) will arise if an unobserved variable is correlated to both a covariate and a flow index. For instance, local topographic features may affect both the annual rainfall and the average streamflow in mountainous regions. Violation of the second assumption leads to substantial uncertainty in the interpolation of the flow indices in Nepal and drives the prediction errors of the statistical approach, as shown in Section S2 of the supplementary materials.

While the performance of the process-based model is also driven by parameter estimation uncertainties, these errors arise from simplifying assumptions about local hydrological processes (rather than uncertainties from their statistical interpolation from neighboring gauges). Additional cross-validation analyses (shown in Section S2 of the supplementary material) suggest that uncertainties

caused by the aggregation of observed point-rainfall statistics at the catchment level drive prediction errors of high flow quantiles. While increasingly accurate remote sensing rainfall data will progressively allow such spatial heterogeneities to be resolved, current precipitation products (e.g., TRMM 3B42) remain substantially biased in mountainous regions like Nepal, where they do not outperform available rain gauges in predicting the frequency and intensity of areal rainfall (Müller and Thompson, 2013). A second source of error arises from the simplifying assumptions made about streamflow recession that do not hold perfectly in the observed catchments. Because they describe the same watershed, the wet and dry recession parameters are assumed to be physically related. In Müller et al. (2014), the scale parameter of the non-linear seasonal recession ( $a$ ) is expressed as an explicit function of the two recession parameters ( $k$  and  $b$ ) for sufficiently short recession times, where power-law recessions can be approximated by exponential functions. We show in Supplementary Materials (Section S2) that, although this approach provides more accurate estimates of  $a$  than would be obtained through spatial interpolation, estimation uncertainties remain, propagate through the model and result in prediction errors during the dry season.

#### 4.1.2 Applicability beyond Nepal

This study compares two specific methods on their ability to predict FDCs in the particular context of ungauged Nepalese basins. Results are thus not necessarily representative of the relative performance of process-based and statistical methods in general, particularly in regions where abundant field data allow more advanced statistical approaches to be implemented. Yet fundamentally, the statistical model relies on observed correlations, rather than assumptions about hydrologic mechanisms. Because FDC shapes are modeled non-parametrically, the approach is applicable to regions with highly variable catchment responses. However, prediction performance in ungauged basins is constrained by interpolation errors in the mean flow. This makes the method unsuitable for regions where the local determinants of mean flow (i.e. rainfall, evapotranspiration, glacial melt) cannot be accurately monitored at the catchment level. In contrast, a key advantage of the process-based model is its ability to exploit characteristics of the stochastic structure of rainfall that can be estimated from daily rainfall observations. The model is appropriate for regions where the spatial heterogeneity of runoff is driven by rainfall, and where the frequency and intensity of rainfall depths at the catchment level can be readily estimated (i.e. small catchments with numerous rain gauges, or places where satellite observations provide a good representation of rainfall statistics). Unlike rainfall, recession behavior arises from lumped and complex interactions between climate, vegetation and groundwater processes that typically cannot be monitored in a spatially explicit manner. The process-based model is therefore inappropriate for regions where the hydrologic response of the catchment is the main source of runoff heterogeneity, or where the assumed recession behavior (in particular the relation between  $a$ ,  $k$  and  $b$ ) does not occur.



Conveniently, the appropriate implementation contexts for both methods appear to be complementary, and the optimal method in a given region is determined by the driving source of runoff heterogeneity in the catchments. Ultimately, the performance of both methods is constrained by their ability to estimate their parameters in ungauged basins. This relation is apparent in Figure 4, where drops in prediction performances correspond to increases in the estimation uncertainty of model parameters. Under these conditions, the performance of each method is driven by the ability of the available observations to capture the variability of the model parameters. When interpolated from neighboring gauges, uncertainties are governed by the interplay between the layout of the gauges and the spatial correlation range of the considered model parameter. When estimated from short observation records, accuracy is determined by the extent to which the available record is representative of the temporal variability of the parameter. These interactions between data availability and runoff variability are inherently local and will affect the determination of the most appropriate method for any given region.

## 4.2 Prediction under Change

Expected shifts in the frequency and intensity of Monsoon rainfall over Nepal only have a marginal impact on the streamflow distributions in the Chepe Kohla catchment, as shown by the numerical simulation presented in (Figure 5 (a, dashed curve)). Consequently, changes in rainfall regime do not appear to affect the performance of either model (Figure 5 (b)), unless they are significantly larger than expected. Climate change may nonetheless affect flow predictions elsewhere. It is therefore helpful to consider the conditions under which FDCs can be reliably predicted in a changing climate.

Although rainfall stationarity is an inherent assumption of the process-based approach, climate change can be incorporated by updating the relevant parameters to their future value to predict the (pseudo-) stationary future state of the system. The method accounts for otherwise confounding changes in the frequency and intensity of rainfall, which are expected in Nepal. By explicitly accounting for soil moisture dynamics and recession behavior, the model emulates the (causal) effect of rainfall on streamflow. As a result, the method reliably predicts the distribution of future streamflow, provided that governing flow generation processes are in line with the basic assumptions listed in Section 2.1.1.

In contrast, the statistical model is solely based on observed correlations, leading to two important sources of errors for predictions under change. First, the model only accommodates rainfall changes to the extent that the estimated statistical relation between rainfall and runoff is representative of local runoff coefficients. The model will not reliably predict future streamflows if runoff coefficients are strongly spatially heterogeneous, or if the cross sectional sample of gauges fails to capture important processes governing mean flow. This source of uncertainty appears to be significant in Nepal, as illustrated by the substantial bias in annual flow predictions on Figure 5(c). Secondly, the statistical model only considers the effect of *average* rainfall on *average* flow: the effect of rainfall *distribution*

in streamflow *distribution* is ignored. As a result, the model cannot predict changes in the shape of FDC that are brought about by changing rainfall. The prediction performance of the statistical approach is therefore determined by the resilience of the flow regime, that is the extent to which streamflow distribution is affected by shifting rain signals (Botter et al., 2013): the method will perform poorly in catchments with non-resilient flow regimes. The Monte Carlo analysis presented in Supplementary Materials (Sections S3 and S4) shows that streamflow resilience in seasonally dry catchments depends on two distinct seasonal effects: a 'direct' effect driven by the ratio between  $\lambda_P$  and  $k$  during the wet season, and an 'indirect' effect during the dry season, when resilience is determined by the interplay between  $Q_0$  (i.e. wet-season rainfall) and  $b$ . In seasonally dry climates, we expect the statistical method to be most reliable in regions where wet seasons are short with limited total rainfall but persistent flow regimes, and where the recession behavior during the dry-season is close to linear.

Lastly, a key assumption in this study is that catchment response (in terms of low-flow or recession characteristics) is independant of climate. It is possible that shifts in climate have an effect on catchment response by affecting the partitionning of effective rainfall between storage and runoff. Although not quantitatively assessed in this study, we expect that this effect would negatively affect the performance of both approaches.

## 5 Conclusions

Stochastic, process-based models predicted the FDCs for ungauged catchments in Nepal well, with a performance that was comparable to that of statistical models. It suggests that in regions with globally representative gauge-densities, and under seasonally dry climates, the advantages of the statistical approaches relative to stochastic models noted in previous analyses (Blöschl et al., 2013) may not apply. Fundamentally, the performances of both approaches are strongly affected by the method chosen to estimate model parameters in ungauged basins, so this conclusion comes with the caveat that this study cannot be interpreted as a general benchmark to compare these approaches at a global level. Although we believe that the selected models are appropriate to compare process-based and statistical approaches for practical PUB application in Nepal, their relative performance may be different in other regions, where more abundant information on catchment characteristics allow more complex (and presumably more accurate) regionalization approaches to be applied. Thus, substantial research remains to be done to compare these approaches in other parts of the world, where locally appropriate methods should be carefully considered.

Nonetheless, this study finds a complementarity between the different sources of uncertainty in the stochastic and statistical methods. This suggests that model selection should be driven by a consideration of the main drivers of heterogeneity in any study catchment: Process-based models are advisable if climate is likely to be the main source of runoff heterogeneity. Conversely, statistical

555 methods are more appropriate for regions with substantially different recession behaviors across catchments. These distinctions provide a potentially robust basis for model selection in any given application.

The results also suggest that the sensitivity of statistical approaches to changes in rainfall statistics is dependent on the ‘resilience’ of the flow regime as defined by Botter et al. (2013). Overall, the process-based models are more reliable in projecting FDCs into new rainfall regimes. This is particularly true for catchments characterized by a strong wet-season runoff and a rapid, strongly non-linear hydrologic response, because their flow regime is particularly vulnerable to rainfall changes, making the assumptions of the statistical model inappropriate.

The excellent performance of both process-based and statistical models for the FDC and PDF in ungauged basins suggests that extending probabilistic analyses in such basins to also include flow-derived variables such as hydropower capacity (Basso and Botter, 2012) or ecological responses (Thompson et al., 2013a) may be feasible. While these prospects are enticing, we note that a model’s ability to predict an FDC with high fidelity is not necessarily indicative of prediction performances on all derived stochastic properties. For instance, Dralle et al. (2015) demonstrate that the crossing properties of streamflow can be very poorly estimated by stochastic process-based models, even in applications where the same models predict the PDF of flow well. Further exploration of the potential opportunities and limitations afforded by use of probabilistic models in ungauged basins offers a promising avenue for future study.

## Appendix A: Process-based streamflow distribution model for seasonally dry climates

This appendix presents the analytical expression of FDC in seasonal climates derived in Müller et al. (2014). The approach assumes that rainfall can be represented as a marked Poisson process with exponentially distributed depths. Catchments are modeled as spatially homogenous linear reservoirs with linear evapotranspiration losses. Under these conditions, wet season streamflow can be represented as a gamma-distributed random variable (Botter et al., 2007b):

$$Q_w \sim \text{Gamma}(m, \alpha_Q^{-1})$$

575 with  $m = \lambda/k$  and  $\alpha_Q = \alpha_P k A$ , and where  $k$  is the linear recession constant,  $A$  the area of the contributing catchment and  $\alpha_P$  the mean intensity of wet season rainfall. The frequency  $\lambda$  of runoff events can be expressed as a function of the frequency ( $\lambda_P$ ) and intensity of rainfall (Botter et al., 2007b):

$$\lambda = \eta \frac{\exp(-\gamma) \gamma^{\frac{\lambda_P}{\eta}}}{\Gamma_L(\lambda_P/\eta, \gamma)} \quad (\text{A1})$$

580 where  $\Gamma_L(\cdot, \cdot)$  is the lower incomplete gamma function, and where  $\eta = ET/SSC$  and  $\gamma = SSC/\alpha_P$  are respectively the ratio between maximum evapotranspiration and soil storage capacity, and the ratio between soil storage capacity and mean rainfall intensity.

Dry season streamflow is modeled as a seasonal recession starting at the last discharge peak of the wet season. Because wet season streamflow is a gamma-distributed variable, streamflow at discharge peaks, and therefore the initial condition of the seasonal recession, is itself a gamma distributed variable (Müller et al., 2014):

$$Q_{peak} \sim \text{Gamma}(m+1, \alpha_Q^{-1}).$$

Assuming a power law-relation between discharge and recession rate, the cumulative distribution function of dry season streamflow can be expressed as (Müller et al., 2014):

$$585 \quad P_{Q_d}(Q) = \begin{cases} 1 + \frac{q_d^r \Gamma_1 - \alpha_Q^r \Gamma_2}{arT_d \Gamma(m+1)}, & \text{if} \\ & Q > -(arT_d)^{\frac{1}{r}} \\ & \text{and } r < 0 \\ 1 + \frac{q_d^r \Gamma_1 - \alpha_Q^r \Gamma_2}{arT_d \Gamma(m+1)} + \frac{\alpha_Q^r \Gamma_4 + (Q^r - arT_d) \Gamma_3}{arT_d \Gamma(m+1)}, & \text{otherwise} \end{cases}$$

with

$$\begin{aligned} \Gamma_1 &= \Gamma_U(m+1, \alpha_Q^{-1}Q) \\ \Gamma_2 &= \Gamma_U(r+m+1, \alpha_Q^{-1}Q) \\ \Gamma_3 &= \Gamma_U\left(m+1, \alpha_Q^{-1}(Q^r + arT_d)^{\frac{1}{r}}\right) \\ 590 \quad \Gamma_4 &= \Gamma_U\left(r+m+1, \alpha_Q^{-1}(Q^r + arT_d)^{\frac{1}{r}}\right) \end{aligned}$$

$\Gamma(\cdot)$  and  $\Gamma_U(\cdot, \cdot)$  denote the complete and upper incomplete gamma functions;  $T_d$  is the duration of the dry season;  $r = 1 - b$  and  $a$  are the parameters of the non-linear recession, which are assumed stationary. Because they describe the same watershed, recession parameters for the wet and dry seasons are related. If power-law recessions can be approximated by an exponential function for  
595 sufficiently short recession times, we can express  $a$  as a function of  $k$  and  $b$  (Müller et al., 2014):

$$a \approx \frac{\lambda}{-r} \left( e^{\frac{-r}{m}} - 1 \right) (\alpha_Q \cdot (m+1)) \quad (\text{A2})$$

The law of total probability can finally be used to combine seasonal streamflow distributions and derive the cumulative distribution function of streamflow for the whole year:

$$P_Q(Q) = \left(1 - \frac{T_d}{365}\right) \cdot P_{Q_w}(Q) + \frac{T_d}{365} \cdot P_{Q_d}(Q) \quad (\text{A3})$$

600 The FDC for seasonally dry climates is finally obtained by plotting the streamflow quantiles  $Q$  against  $1 - P_Q(Q)$ , the complement of the the cumulative distribution function of streamflow.

*Acknowledgements.* The Swiss National Science Foundation are gratefully acknowledged for funding (M.F.M).

## References

- Alaouze, C. M.: Reservoir Releases to Uses with Different Reliability Requirements, *AWRA Water Resources Bulletin*, 25, 1163–1168, 1989.
- Alternative Energy Promotion Center: Construction and Installation Manual for Micro hydropower Project Installers (In Nepalese), Government of Nepal, 2014.
- Arora, M., Goel, N., Singh, P., and Singh, R.: Regional flow duration curve for a Himalayan river Chenab., *Nordic hydrology*, 36, 193–206, 2005.
- Basso, S. and Botter, G.: Streamflow variability and optimal capacity of run-of-river hydropower plants, *Water Resources Research*, 48, doi:10.1029/2012WR012 017, 2012.
- Bélisle, C. J.: Convergence theorems for a class of simulated annealing algorithms on  $\mathbb{R}^d$ , *Journal of Applied Probability*, 29, 885–895, 1992.
- Blöschl, G., Sivapalan, M., Wagener, T., Viglione, A., and Savenije, H.: *Runoff Prediction in Ungauged Basins: Synthesis across Processes, Places and Scales*, Cambridge University Press, 2013.
- Botter, G., Peratoner, F., Porporato, A., Rodriguez-Iturbe, I., and Rinaldo, A.: Signatures of large-scale soil moisture dynamics on streamflow statistics across US climate regimes, *Water Resources Research*, 43, doi:10.1029/2007WR006 162, 2007a.
- Botter, G., Porporato, A., Rodriguez-Iturbe, I., and Rinaldo, A.: Basin-scale soil moisture dynamics and the probabilistic characterization of carrier hydrologic flows: Slow, leaching-prone components of the hydrologic response, *Water Resources Research*, 43, doi:10.1029/2006WR005 043, 2007b.
- Botter, G., Porporato, A., Rodriguez-Iturbe, I., and Rinaldo, A.: Nonlinear storage-discharge relations and catchment streamflow regimes, *Water resources research*, 45, doi: 10.1029/2008WR007 658, 2009.
- Botter, G., Basso, S., Rodriguez-Iturbe, I., and Rinaldo, A.: Resilience of river flow regimes, *Proceedings of the National Academy of Sciences*, 110, doi: 10.1073/pnas.1311920 110, 2013.
- Brutsaert, W. and Nieber, J. L.: Regionalized drought flow hydrographs from a mature glaciated plateau, *Water Resources Research*, 13, doi: 10.1029/WR013i003p00 637, 1977.
- Castellarin, A., Galeati, G., Brandimarte, L., Montanari, A., and Brath, A.: Regional flow-duration curves: reliability for ungauged basins, *Advances in Water Resources*, 27, doi:10.1016/j.advwatres.2004.08.005, 2004a.
- Castellarin, A., Vogel, R., and Brath, A.: A stochastic index flow model of flow duration curves, *Water Resources Research*, 40, doi:10.1029/2003WR002 524, 2004b.
- Castellarin, A., Botter, G., Hughes, D., Liu, S., Ouarda, T., Parajka, J., Post, D., Sivapalan, M., Spence, C., Viglione, A., and Vogel, R.: *Runoff prediction in ungauged basins: Synthesis across processes, places and scales. Chapter 7: Prediction of Flow Duration Curves in Ungauged Basins*, Cambridge University Press, 2013.
- Ceola, S., Botter, G., Bertuzzo, E., Porporato, A., Rodriguez-Iturbe, I., and Rinaldo, A.: Comparative study of ecohydrological streamflow probability distributions, *Water Resources Research*, 46, doi: 10.1029/2010WR009 102, 2010.
- Chalise, S., Kansakar, S., Rees, G., Croker, K., and Zaidman, M.: Management of water resources and low flow estimation for the Himalayan basins of Nepal, *Journal of Hydrology*, 282, doi:10.1016/S0022–1694(03)00 250–6, 2003.

- Cheng, L., Yaeger, M., Viglione, A., Coopersmith, E., Ye, S., and Sivapalan, M.: Exploring the physical controls of regional patterns of flow duration curves—Part 1: Insights from statistical analyses, *Hydrology and Earth System Sciences*, 16, doi:10.5194/hess-16-4435-2012, 2012.
- 645 Chitrakar, P.: Micro-hydropower design aids manual, Small Hydropower Promotion Project (GTZ) and Mini-grid support program (Alternate Energy Promotion Center, Government of Nepal), 2004.
- Coopersmith, E., Yaeger, M., Ye, S., Cheng, L., and Sivapalan, M.: Exploring the physical controls of regional patterns of flow duration curves—Part 3: A catchment classification system based on regime curve indicators, *Hydrology and Earth System Sciences*, 16, doi:10.5194/hess-16-4467-2012, 2012.
- 650 Department of Hydrology and Meteorology: Daily Streamflow and Precipitation Data,, Kathmandu, 2011.
- Doulatyari, B., Betterle, A., Basso, S., Biswal, B., Schirmer, M., and Botter, G.: Predicting streamflow distributions and flow duration curves from landscape and climate, *Advances in Water Resources*, 83, doi:10.1016/j.advwatres.2015.06.013, 2015.
- Dralle, D. N., Karst, N., and Thompson, S.: Dry season streamflow persistence in seasonal climates, *Water Resources Research*, In Press, doi:10.1002/2015WR017752, 2015.
- 655 Global Runoff Data Center: Global Runoff Data Base, Global Runoff Data Centre. Koblenz, Federal Institute of Hydrology (BfG), 2014.
- Greene, W. H.: *Econometric analysis*, Pearson Education India, 2003.
- HKH-FRIEND: Hindu Kush Himalayan - Flow Regimes from International Experimental and Network Data, UNESCO International Hydrological Programme, 2004.
- 660 Hughes, D. and Smakhtin, V.: Daily flow time series patching or extension: a spatial interpolation approach based on flow duration curves, *Hydrological Sciences Journal*, 41, 851–871, 1996.
- Lambert, L. and Chitrakar, B.: Variation of potential evapotranspiration with elevation in Nepal, *Mountain Research and Development*, pp. 145–152, 1989.
- 665 Lazzaro, G., Basso, S., Schirmer, M., and Botter, G.: Water management strategies for run-of-river power plants: Profitability and hydrologic impact between the intake and the outflow, *Water Resources Research*, 49, doi:10.1002/2013WR014210, 2013.
- Milly, P., Julio, B., Malin, F., Robert, M., Zbigniew, W., Dennis, P., and Ronald, J.: Stationarity is dead, *Science*, 319, doi:10.1126/science.1151915, 2008.
- 670 Montanari, A., Young, G., Savenije, H., Hughes, D., Wagener, T., Ren, L., Koutsoyiannis, D., Cudennec, C., Toth, E., and Grimaldi, S.: Panta Rhei—Everything Flows: Change in hydrology and society—The IAHS Scientific Decade 2013–2022, *Hydrological Sciences Journal*, 58, doi:10.1080/02626667.2013.809088, 2013.
- Mu, X., Zhang, L., McVicar, T. R., Chille, B., and Gau, P.: Analysis of the impact of conservation measures on stream flow regime in catchments of the Loess Plateau, China, *Hydrological Processes*, 21, doi:10.1002/hyp.6391, 2007.
- 675 Müller, M. F. and Thompson, S. E.: Bias adjustment of satellite rainfall data through stochastic modeling: Methods development and application to Nepal, *Advances in Water Resources*, 60, doi:10.1016/j.advwatres.2013.08.004, 2013.

- 680 Müller, M. F. and Thompson, S. E.: TopREML: a topological restricted maximum likelihood approach to regionalize trended runoff signatures in stream networks, *Hydrology and Earth System Sciences*, 19, doi:10.5194/hess-19-2925-2015, 2015.
- Müller, M. F., Dralle, D. N., and Thompson, S. E.: Analytical model for flow duration curves in seasonally dry climates, *Water Resources Research*, 50, doi:10.1002/2014WR015301, 2014.
- 685 Müller, M. F.: Bridging the Information Gap: Remote Sensing and Micro Hydropower Feasibility in Data-Scarce Regions, Doctoral Dissertation, University of California, Berkeley, CA, 2015.
- Muneepeerakul, R., Azale, S., Botter, G., Rinaldo, A., and Rodriguez-Iturbe, I.: Daily streamflow analysis based on a two-scaled gamma pulse model, *Water Resources Research*, 46, doi: 10.1029/2010WR009286, 2010.
- 690 NASA Land Processes Distributed Active Archive Center (LP DAAC): ASTER GDEM v2, NASA Land Processes Distributed Active Archive Center (LP DAAC). ASTER L1B. USGS/Earth Resources Observation and Science (EROS) Center, Sioux Falls., 2011.
- Nathan, R. and McMahon, T.: Evaluation of automated techniques for base flow and recession analyses, *Water Resources Research*, 26, 1465–1473, 1990.
- 695 Sauquet, E. and Catalogne, C.: Comparison of catchment grouping methods for flow duration curve estimation at ungauged sites in France, *Hydrology and Earth System Sciences*, 15, doi:10.5194/hess-15-2421-2011, 2011.
- Schaefli, B., Rinaldo, A., and Botter, G.: Analytic probability distributions for snow-dominated streamflow, *Water Resources Research*, 49, doi:10.1002/wrcr.20234, 2013.
- 700 Searcy, J. and Hardison, C.: Double-mass curves. *Manual of hydrology: Part I, General surface water techniques*, US Geol Surv Water Supply Paper, 1960.
- Shao, J. and Tu, D.: *The Jackknife and Bootstrap*, Springer-Verlag, New York, 2012.
- Shrestha, D. P.: Assessment of soil erosion in the Nepalese Himalaya: a case study in Likhu Khola Valley, Middle Mountain Region, *Land Husbandry*, 2, 59–80, 1997.
- 705 Stokstad, E.: Scarcity of rain, stream gages threatens forecasts, *Science*, 285, doi: 10.1126/science.285.5431.1199, 1999.
- Thompson, S., Levin, S., and Rodriguez-Iturbe, I.: Linking plant disease risk and precipitation drivers: a dynamical systems framework, *The American Naturalist*, 181, doi: 10.1086/668572, 2013a.
- Thompson, S., Sivapalan, M., Harman, C., Srinivasan, V., Hipsey, M., Reed, P., Montanari, A., and Blöschl, G.:  
710 Developing predictive insight into changing water systems: use-inspired hydrologic science for the Anthropocene, *Hydrology and Earth System Sciences*, 17, doi: 10.5194/hess-17-5013-2013, 2013b.
- Turner, A. G. and Annamalai, H.: Climate change and the South Asian summer monsoon, *Nature Climate Change*, 2, doi:10.1038/nclimate1495, 2012.
- Turner, A. G. and Slingo, J. M.: Subseasonal extremes of precipitation and active-break cycles of the Indian  
715 summer monsoon in a climate-change scenario, *Quarterly Journal of the Royal Meteorological Society*, 135, 549–567, 2009.
- United States Geological Survey: USGS Threatened and Endangered Streamgages, [http://streamstats09.cr.usgs.gov/ThreatenedGages/ThreatenedGages\\_str.html](http://streamstats09.cr.usgs.gov/ThreatenedGages/ThreatenedGages_str.html), 2015.

- 720 Vogel, R. and Fennessey, N.: Flow-duration curves. I: New interpretation and confidence intervals, *Journal of Water Resources Planning and Management*, 120, 485–504, 1994.
- Westerberg, I. K., Gong, L., Beven, K. J., Seibert, J., Semedo, A., Xu, C.-Y., and Halldin, S.: Regional water balance modelling using flow-duration curves with observational uncertainties, *Hydrology and Earth System Sciences*, 18, 2993–3013, 2014.



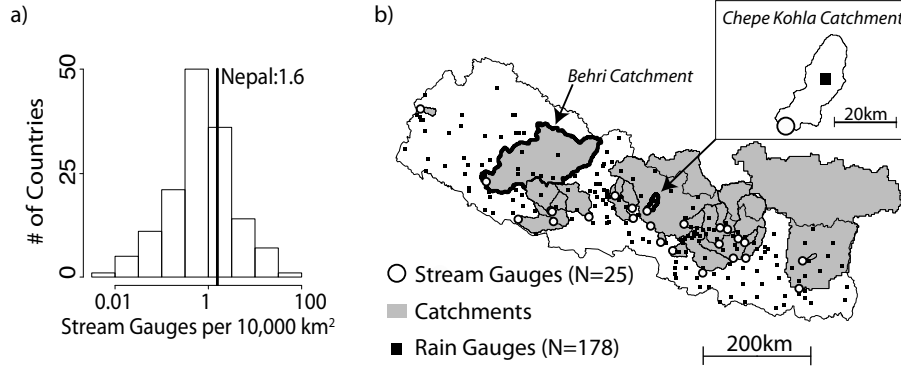


**Figure 1.** (a) Global histogram of the approximate spatial density of streamflow gauges by nation, represented by the sample of 8540 gauges indexed by the Global Runoff Data Center for 146 countries (Global Runoff Data Center, 2014). With a density of 1.6 gauges per 10,000  $km^2$ , Nepal falls close to the mode of the global distribution. (b) Location of the rain gauges, streamflow gauges and corresponding Nepalese catchments used in the analysis.

**Table 1.** Catchment characteristics. Median values and interquartile distances (IQD) are given for the whole sample of 25 gauges. The table also presents characteristics of the Chepe Kohla watershed considered in the analysis as a case study.

	Streamflow:		Topography:				Climate:						Recession:			
	$Q_m$	$q_{95}$	$N_y$	$A$	$z_m$	$z_M$	$P_y$	$T_{\text{mons}}$	$\lambda_P$	$\alpha_P$	$AR$	$CV$	$ET$	$k$	$b$	
All gauges																
<i>Median</i>	76.1	0.14	22	1355	481	5209	1952	99	0.71	18.8	0.29	0.92	2.5	0.17	2.38	
<i>Min</i>	7.3	0.06	10	130	116	1913	1260	88	0.54	12.1	0.09	0.61	0.40	0.07	1.99	
<i>Max</i>	1462.4	0.25	41	32817	1641	8369	4030	152	0.91	33.0	0.51	1.53	3.27	0.32	2.99	
Chepe Kohla	23.0	0.14	31	277	475	4711	3050	100	0.84	26.5	0.09	1.03	2.1	0.20	2.41	

$Q_m$  is mean annual flow in  $m^3 s^{-1}$ ;  $q_{95}$  is the 95<sup>th</sup> flow percentile normalized by  $Q_m$ ;  $N_y$  indicates the number of observation years;  $A$  is the catchment area in  $km^2$ ;  $z_m$  and  $z_M$  are respectively the minimum and maximum elevation of the basins meters;  $P_y$  is mean precipitation in  $mm/y$ ;  $T_{mons}$  is the estimated duration of the monsoon in days;  $\lambda_P$  is rainfall frequency during the monsoon (in  $d^{-1}$ );  $\alpha_P$  is mean rainfall intensity in  $mm/d$ ;  $AR$  is the first-order autocorrelation coefficient of rainfall occurrence ( $AR = 0$  if rainfall follows a Poissonian process),  $CV$  is the coefficient of variation of rainfall intensity on rainy days ( $CV=1$  if depths are exponentially distributed);  $ET$  [mm/d] is the reference evapotranspiration during the rainy season Lambert and Chitrakar (1989);  $k$  is the linear recession constant estimated during the monsoon (in  $d^{-1}$ ) and  $b$  is the non linear exponent of the seasonal recession. A soil moisture capacity of 16mm are assumed throughout the country (Müller et al., 2014).

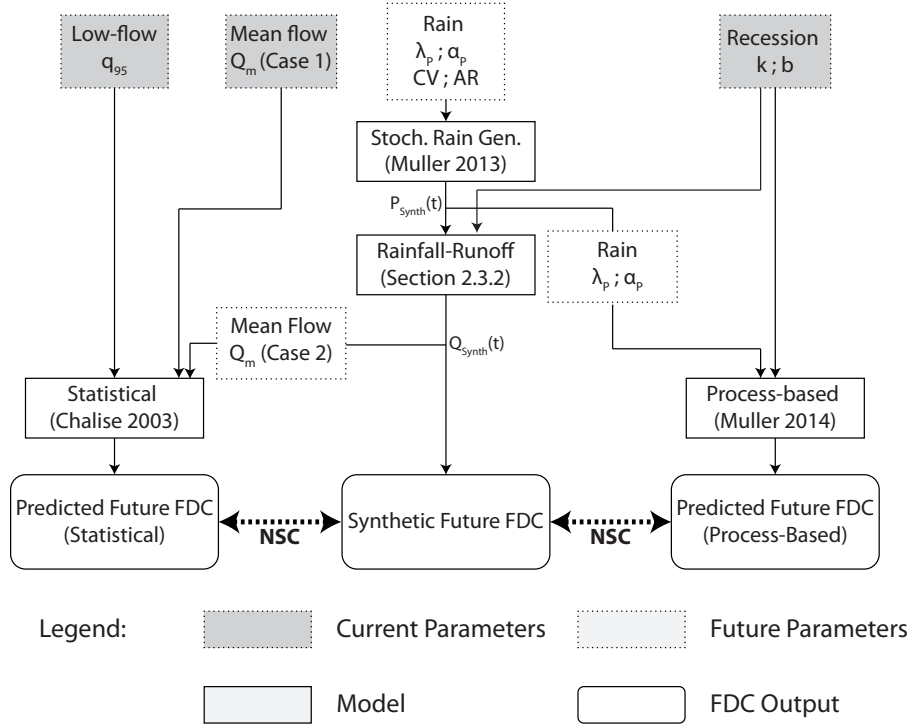


**Figure 2.** Numerical simulation analysis to assess predictions under change. Future rainfall characteristics (frequency  $\lambda_P$ , mean intensity  $\alpha_P$ , auto-correlation coefficient  $AR$  and coefficient of variation  $CV$ ) are determined according to expected changes in rain regimes in Nepal (see Section 2.3.2), and fed into a stochastic rainfall generator. The resulting 1000 years of synthetic daily rainfall values ( $P_{Synth}(t)$ ) are fed into a rainfall-runoff model that simulates the processes described in Section 2.1.1. The rainfall-runoff model uses current recession, soil and evapotranspiration conditions observed at the Chepe Kohla catchment. The resulting 1000 years of synthetic daily flow values ( $Q_{Synth}(t)$ ) are then reordered to construct an empirical synthetic (future) FDC, which was compared (in terms of the Nash Sutcliffe Coefficient) to modeled FDCs predicted by the statistical and process-based models. The process-based model admits *current* recession conditions, but *future* estimates for rainfall frequency ( $\lambda_P$ ) and mean intensity ( $\alpha_P$ ). Note that unlike the numerically generated empirical FDC, the process-based model assumes Poissonian rainfall with exponentially distributed depths, that is  $CV = 1$  and  $AR = 0$ . Current low flow characteristics ( $q_{95}$ ) are fed into the statistical model, as well as the current or future (i.e. computed from synthetic streamflow time series) mean flow, depending on the extent to which mean rainfall is an unbiased predictor of mean flow (Cases 1 and 2 described in Section 2.3.2).

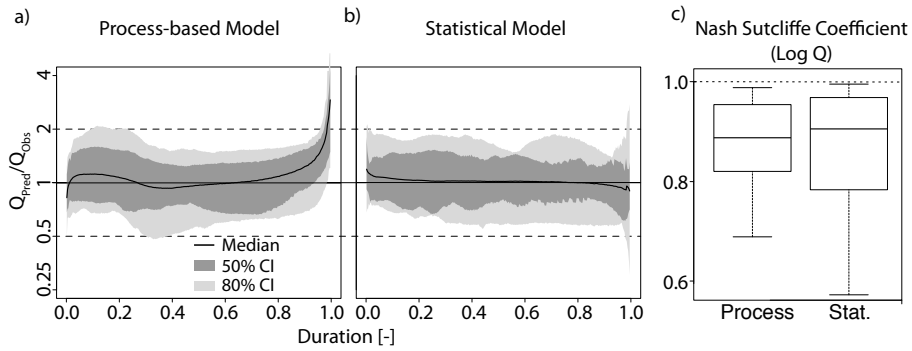


**Figure 3.** Flow duration curve prediction performance in ungauged basins. The error duration curves of the leave-one-out cross-validation analysis using the process-based and statistical models are presented in panels (a) and (b) respectively. Relative errors are plotted on a log scale in order to allow the graphs to be balanced on the y-axis: a relative prediction error of 2 (the model predicts double the observed value) is at the same distance from  $y=1$  (perfect prediction) than a relative error of  $1/2$  (the model predicts half the observed value). Durations are plotted on the x-axis, with  $x=0$  and  $x=1$  for the highest and lowest flow quantiles respectively. Panel (c) shows box plots of Nash Sutcliffe coefficients computed from log-transformed flow quantiles.

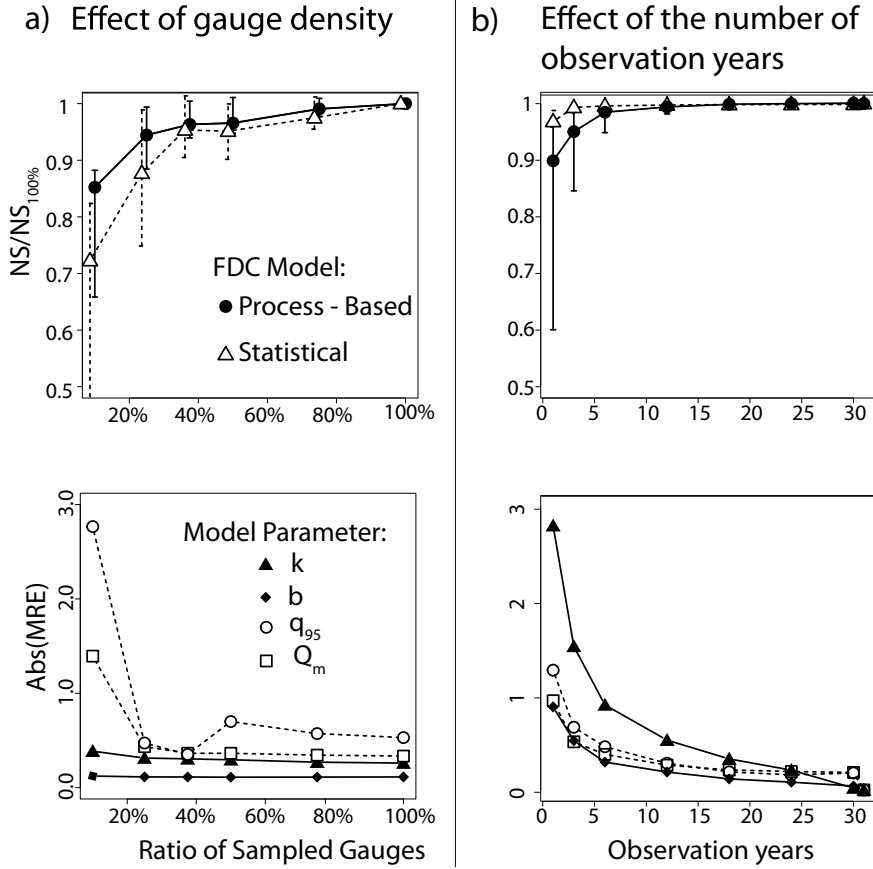


**Figure 4.** Sensitivity of models to data scarcity. (a) Cross-validation analysis showing the sensitivity of both models to a decreasing number of calibration gauges. (b) Resampling analysis of streamflow observations in the Chepe Kohla (N=10,000) catchment showing the effect of the number of observation years. In panels (a) and (b), the effects on FDC prediction performances (top) are shown by plotting the ratio of calibration gauges sampled (or the number of observation years) against the relative Nash Sutcliffe coefficient (with the NSC for the full set of available data as reference). The plot shows the median value for all iterations, and the error bars indicate the interquartile (25 - 75%) range. The prediction uncertainties of model parameters (bottom) are given in absolute values of relative prediction errors.

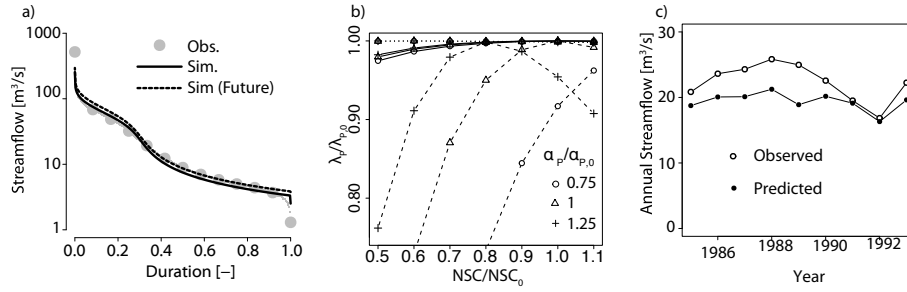


**Figure 5.** Sensitivity of models to changes in the precipitation regime. (a) Empirical and simulated flow duration curves at Chepe Kohla. The simulated FDC obtained from the stochastic rainfall generator and the bucket watershed model (solid) reproduces the empirical FDC constructed from the observed streamflow well (grey dots). Rainfall changes expected in Nepal ( $\alpha_P/\alpha_{P,0} = 1.2$ ,  $\lambda_P/\lambda_{P,0} = 0.98$ ) do not have a substantial influence on the simulated flow distribution (dashed).  $\alpha_P$  and  $\lambda_P$  designate the mean depth and frequency of wet season rainfall, respectively. (b) Sensitivities to relative changes in rainfall frequency and intensity over the Chepe Kohla catchment. The performance of the process-based model is not affected by rainfall changes (dotted). The sensitivity of the statistical model depends on its ability to predict changes in mean flow from annual rainfall. The model is highly sensitive to rain changes if average streamflow cannot be predicted (dashed), and is robust to moderate changes if average flow is perfectly predicted (solid). (c) The linear regression of the statistical model underestimates annual flows at the Chepe Kohla when using a cross-sectional sample (25 gauges) to estimate the local relation between average rainfall and average runoff.

# Supplementary Materials: Comparing statistical and process-based flow duration curve models in ungauged basins and changing rain regimes

Marc F. Müller, Sally E. Thompson\*

January 2016

This document contains the supplementary material to the research article *Comparing statistical and process-based flow duration curve models in ungauged basins and changing rain regimes* by M.F. Müller and S.E. Thompson (2016), published in *Hydrology and Earth System Science*. Section S1 describes the performance of the Medium Irrigation Project method currently implemented in Nepal to predict Flow Duration Curves (FDC) in ungauged basins for infrastructure design purposes. Section S2 describes supplementary cross-validation analyses conducted to attribute the uncertainty sources of the assessed methods. Section S3 describes the theoretical arguments relating catchment characteristics to the resilience of stream regimes (and therefore the reliability of the statistical method for predictions under change) in seasonally dry climates. Lastly, Section S4 describes the Monte Carlo analysis conducted to test these hypothesized relations.

## **S1 Performance of the Medium Irrigation Project method in ungauged Nepalese basins**

To benchmark the methods evaluated in this study, we assess the predictive performance of the Medium Irrigation Project, an empirical method currently used to predict streamflow distribution in small mountainous catchments in Nepal for infrastructure design purposes. The method is prescribed by official micro hydropower design guidelines in Nepal Alternative Energy Promotion Center [1]. The approach, described in [3], divides Nepal into seven hydrologic regions characterized by different sets of monthly

---

\*Department of Civil and Environmental Engineering, Davis Hall, University of California, Berkeley CA, USA

flow indices. Streamflow distribution in ungauged catchments is determined by performing a site visit in mid-April to evaluate discharge under low-flow conditions. In our validation analysis, we emulated this step by selecting the daily flow measured on April 15<sup>th</sup> of a randomly drawn observation year at each gauge. The measured flow is then used to scale the regional monthly indices corresponding to the location of the catchment. All regions have an index of 1 for the month of April (when low-flow conditions are observed), and larger indices for the other months. FDCs can finally be computed by reordering daily flow values interpolated from the obtained monthly flows.

A fundamental flaw of the method is that it assumes that discharge measured in mid-April on a given year is representative of lowest flow conditions that can be observed in the catchment. This assumption does not hold if effective rain events have occurred shortly before discharge was measured or, more to the point, if the current year is not a particularly dry year. As a result, predicted FDCs substantially overestimate observed flows, as shown in Figure S1 (a), and provide a clear motivation to seek improved, yet tractable prediction options.

## **S2 Determination of Uncertainty Sources: Supplementary Analyses**

### **S2.1 Statistical Method**

Figure S1 (b) shows that parameter interpolation errors are the main source of uncertainty of the statistical method. Using observed (instead of predicted) flow indices substantially reduces the width of the error-duration curve of the statistical method. The relative sensitivity of the statistical method to interpolation errors in each flow index was evaluated through a numerical simulation (Figure S2 (a)). The prediction performance was more sensitive to errors in  $Q_m$  than  $q_{95}$ . This is consistent with the fact that, while  $Q_m$  has a direct effect on all the quantiles of the FDC,  $q_{95}$  only determines the type of FDC shape that is selected, and two different values of  $q_{95}$  may generate identical FDC shapes. The statistical approach assumes that catchments with similar low-flow indices ( $q_{95}$ ) have identical hydrological responses, and therefore identical FDC shapes. Errors caused by the violation of this assumption also appear in the error duration curve on Figure S1 (b). The statistical method assigns gauges to a finite number of bins, according to their low flow index, and determines a FDC shape for each bin. The error duration curve shown on Figure S1 (b) represents differences in the FDC shapes of catchments within the bins (i.e. with similar low flow indices). A tradeoff arises in determining the number of bins: a small number of large bins leads to large averaging errors within the bins, while a large number of thin bins increases the model's sensitivity to interpolation errors in  $q_{95}$ .

## S2.2 Process-based Method

In contrast, interpolation uncertainties on the model parameters ( $k$  and  $b$ ) only marginally affect the prediction performance of the process-based approach (Figure S3 (a)). Two other sources of error appear to drive prediction performance. Firstly, uncertainties are caused by the aggregation of point-rainfall statistics to the catchment level. These errors are caused by spatial heterogeneities in wet season rainfall and principally affect high flows, as seen when comparing Figures S3 (b) and (c). Secondly, the numerical analysis presented in Figure S2 illustrates the crucial importance of dry-season recession constants. While the model is remarkably robust to deviations from key assumptions on rainfall distribution and recession relations [see 4], prediction errors at low flows appear to be caused by errors in the determination of  $a$ , the scale parameter of the non-linear seasonal recession (Figure S3 (b)). In Müller et al. [4],  $a$  is expressed as an explicit function of  $k$  and  $b$  for sufficiently short recession times, where power-law recessions can be approximated by exponential functions. Although this approach provides more accurate estimates of  $a$  than would be obtained through spatial interpolation (Figure S3 (b)), estimation uncertainties remain, propagate through the model and drive prediction errors during the dry season.

The numerical analysis presented in Figure S2 illustrates the crucial importance of dry-season recession constants. Unlike the statistical model, the process-based model is affected by errors in both of its parameters ( $k$  and  $b$ ). However, the model's sensitivity to  $k$  is at least partly due to its effect on the estimation of  $a$ . The sensitivity of  $k$  drops if the wet-season recession constant is *not* used to determine  $a$ , as seen in Figure S2 (c), where the error introduced on  $k$  does not propagate to  $a$ . This effect is also visible in the resampling analysis on short time series (Figure 3(c) of the main article), where the uncertainty on  $k$  only marginally affects prediction performance, which declines when  $b$  estimates become inaccurate. This shows that the performance of the model is strongly driven by the estimation of dry-season recession constants in ungauged catchments.

## S3 Catchment Characteristics and Streamflow Resilience in Seasonally Dry Climates

We examine the linkages between the resilience of flow regimes and the physical characteristics of the catchments. This allows us to identify regions where the statistical method may not provide reliable predictions under change because the flow distribution is vulnerable to changing rainfall. By explicitly representing runoff generation processes, the stochastic dynamic framework used in the process-based model is an ideal tool to explore the resilience of flow regimes in catchments that follow its basic underlying assumptions on recession behavior. A similar model was used in non-seasonal climates by Botter et al. [2] to relate the resilience of the probability density function of streamflow to observable catchment characteristics. Here we discuss the case



of seasonally-dry climates, where the characteristics of the seasonal recessions can substantially affect streamflow resilience, here measured as the change in the flow duration curve (in terms of differences in Nash Sutcliffe Coefficient) resulting from a change in rainfall <sup>1</sup>. We use the relations derived in the stochastic dynamic framework [4] to infer the effect of rainfall and recession characteristics on the resilience of flow regimes. This will allow the reliability of the statistical models to be assessed for predictions under change.

During the wet season, flow regimes are determined by the ratio between  $\lambda$ , the frequency of effective (i.e. runoff-generating) rain events, and  $k$  the (linear) recession constant that represents the time scale of the hydrological response of the catchment [2]. If  $\lambda/k > 1$ , frequent effective rainfall and a slow catchment response guarantee a persistent supply of runoff to the stream. If  $\lambda/k < 1$ , effective rain is not frequent enough to compensate for rapid decreases in streamflow after runoff events, and the stream may become intermittent. Streamflow in persistent regimes ( $\lambda/k > 1$ ) is driven by rainfall, whereas streamflow in intermittent regimes ( $\lambda/k < 1$ ) is constrained by the ability of the catchment to modulate the release of water stored in the subsurface. Accordingly, rainfall changes affect most flow quantiles in the persistent regime and shift the entire flow distribution, but they preferentially affect high flows in the intermittent regime, which occur immediately after effective rain events. As a result, intermittent regimes are more resilient to climate change in terms of the mean effect on the entire streamflow distribution, as observed by Botter et al. [2] and illustrated in Figure S4 (a). However, when specifically considering climate effects on the *shape* of the flow distribution (i.e. by normalizing all flow quantiles by their mean), intermittent regimes are more vulnerable to rainfall changes, which ‘tilt’ normalized FDCs by preferentially affecting high flows (Figure S4 (b)). Consequently, we expect the statistical method to perform better in persistent flow regimes because the shape of streamflow distribution is less sensitive to changing rainfall. This is confirmed in the Monte Carlo analysis presented in below, where the ratio  $\lambda/k$  is positively correlated to the performance of the statistical model.

If no significant rainfall occurs outside of the wet season, climate change only affects dry-season flow through its effect on the initial condition of the seasonal recession. It follows the flow regime will be more sensitive to rainfall changes if the duration of the wet season (when rainfall has a ‘direct’ effect on streamflow) is long and thus affects a greater proportion of the annual flow duration curve. This effect is also visible in the Monte Carlo analysis, where the duration of the wet season ( $T_w$ ) is negatively associated with the performance of the statistical model.

The extent to which changes in the initial condition affect the shape of the seasonal recession during the dry season is determined by the non-linear character of the catchment’s response. This can be seen by using the characteristic time-scale of the

---

<sup>1</sup>This contrasts with Botter et al. [2], who considers the effect of rainfall regime changes on the probability distribution function of streamflow. While the general idea is the same, the numerical results can be different.

recession (here we consider the time necessary to reduce peak flow by  $1/e$ ) to characterize its shape. In linear catchments, the recession takes an exponential form, so the characteristic timescale corresponds to the inverse of the recession constant and is not affected by initial conditions. For non-linear catchments, characteristic time can be derived from Equation 1 in the main article:

$$t_{1/e} = \frac{(1 - e^{-r}) Q_0^r}{ar} \quad (1)$$

with  $r = 1 - b$ . In these nonlinear regimes, the initial conditions  $Q_0$  clearly have an effect on the shape of the recession of non-linear catchment. Taking the derivative of Equation 1 with respect to  $Q_0$  shows that a change in initial flow has a stronger influence on the shape of the recession for low values of  $Q_0$ , as illustrated in Figure S4 (c). Consequently, the sensitivity of the dry season flow regimes to climate change scenarios is expected to be highest in strongly non-linear catchments with limited wet season runoff. Predictions of the FDC using the statistical model for non-stationary rainfall regimes are likely to be poor. In the Monte Carlo analysis below, the performance of the statistical method is significantly worse in strongly non-linear catchments. However, the negative correlation between the linearity of the runoff behavior and the prediction performance is weaker for catchments with high wet-season runoff.

The streamflow resilience in seasonally dry catchments depends on two distinct seasonal effects: a 'direct' effect driven by the ratio between  $\lambda_P$  and  $k$  during the wet season, and an 'indirect' effect during the dry season, when resilience is determined by the interplay between  $Q_0$  (i.e. wet-season rainfall) and  $b$ . Streamflow resilience influences the ability of the statistical method to predict FDCs under change. In seasonally dry climates, we expect the statistical method to be most reliable in regions where wet seasons are short with limited total rainfall but persistent flow regimes, and where the recession behavior during the dry-season is close to linear.

## S4 Monte Carlo Analysis of Flow Regime Resilience

We used a Monte Carlo analysis on numerically generated streamflow to estimate the effect of catchment characteristics on streamflow resilience. In the context of this paper, the resilience of flow regimes to climate change is defined as the robustness of the *shape* of FDCs to shifts in the frequency and intensity of rainfall. The analysis proceeds as follows:

1. Topographic and hydroclimatic characteristics are drawn from uniform distributions as described in Table S1.
2. 1000 years of 'current' synthetic daily streamflows are generated from the drawn parameters using the stochastic rainfall generator and rainfall-runoff model described in Section 2.3.2. of the main article.

3. Randomly drawn multiplicative biases are inserted to the parameters representing frequency and intensity of rainfall ( $\lambda_P$  and  $\alpha_P$ ) to emulate climate change, and 1000 years of 'future' synthetic daily streamflow are generated.
4. Current and future FDCs are constructed empirically from the simulated time series, and normalized by their respective means.
5. Differences in the shape of the flow distributions are quantified by computing the Nash Sutcliffe coefficient on the (log) flow quantiles of the two normalized FDCs.

We repeated the procedure 5000 times and used linear regressions to estimate the effect of catchment characteristics on the resilience of flow regimes, as represented by the Nash Sutcliffe coefficient.

Ordinary least squares estimates of the considered regression models are presented in Table S2. The first column presents direct correlations between catchment characteristics and flow regime resilience and indicate significant positive effects for rainfall frequency and intensity and a negative effect of both recession constants. Regression models shown in columns 2 and 3 test the relations hypothesized in the discussions. As expected, column 2 shows that the  $\lambda/k$  ratio has a positive significant effect on the resilience of flow regimes. In order to avoid colinearity issues, all variables used to construct  $\lambda$  (i.e.  $\lambda_P$  and  $\alpha_P$  in Equation A1 of the main article) were removed from the regression model. The significant negative effect of  $T_w$  on streamflow resilience is consistent with the fact that dry season precipitations are neglected. Consequently, changes in rainfall have a direct effect on wet season flows, while only affecting dry season flows through their effect on the initial conditions of the seasonal recession. Lastly, we use mean wet-season rainfall ( $\lambda_P\alpha_P$ ) as a proxy for the initial conditions of the seasonal recession and assess the effect of its interaction with  $b$  on flow resilience in column 3. As expected,  $b$  is strongly negatively associated to flow resilience but its interaction with  $\lambda_P\alpha_P$  is significantly positive. This is consistent with our hypothesis that the shape of non-linear recessions is more sensitive to climate, especially if the initial flow conditions are low.

## References

- [1] Alternative Energy Promotion Center: Construction and Installation Manual for Micro hydropower Project Installers (In Nepalese), Government of Nepal, 2014.
- [2] Botter, G., Basso, S., Rodriguez-Iturbe, I., and Rinaldo, A.: Resilience of river flow regimes, *Proceedings of the National Academy of Sciences*, 110, doi: 10.1073/pnas.1311920110, 2013.
- [3] Chitrakar, P.: Micro-hydropower design aids manual, Small Hydropower Promotion Project (GTZ) and Mini-grid support program (Alternate Energy Promotion Center, Government of Nepal), 2004.

- [4] Müller, M. F., Dralle, D. N., and Thompson, S. E.: Analytical model for flow duration curves in seasonally dry climates, *Water Resources Research*, 50, doi:10.1002/2014WR015301, 2014.

**Table S1:** Parameters of the Monte Carlo analysis. At each run, all parameters are drawn independently from a uniform distribution of the specified range.

Characteristic	Description	Distribution range
$k^{-1}$ [d]	Mean response catchment response time during the wet season	[1, 10]
$b$ [–]	Exponent parameter of the seasonal recession	[1, 3]
$T_w$ [d]	Wet season duration	[50, 300]
$\lambda_P^{-1}$ [d]	Mean inter-arrival time of wet season rainfall	[1, 10]
$\alpha_P$ [mm/d]	Mean intensity of wet seasonal rainfall	[1, 50]
$\text{Log}_{10}(A)$ [ $\log(\text{km}^2)$ ]	(Log) catchment area	[1, 5]
$r_{\lambda_P}$ [–]	Relative change in rainfall frequency	[–0.9, 0]
$r_{\alpha_P}$ [–]	Relative change in rainfall intensity	[0, 1]

**Table S2:** Linear regression results of the Monte Carlo analysis showing the effect of catchment characteristics on flow resilience. Dependent variables are the Nash Sutcliffe coefficients estimated between the normalized current and future FDCs obtained from the Monte Carlo analysis. Independent variables are constructed from the randomly drawn catchment characteristics listed in Table S1. The first column presents the raw effects of the catchment characteristics on flow resilience. Column 2-3 test the direction and significance of the effects described in Section S3. Superscripted stars describe the significance of the estimated regression coefficients, as described by the  $p$ -value of Student's  $t$  test: \*\*\* indicates a trend different from zero at the 99% confidence level; \*\* and \* indicate confidence levels of 95% and 90% respectively.

	<i>Dependent variable:</i>		
	Nash Sutcliffe Coefficient		
	(Baseline)	(Wet. seas)	(Dry seas.)
$\lambda_P$	$3.17 \cdot 10^{-1***}$ ( $2.07 \cdot 10^{-2}$ )		
$\alpha_P$	$1.49 \cdot 10^{-3***}$ ( $3.27 \cdot 10^{-4}$ )		
$k$	$-4.54 \cdot 10^{-1***}$ ( $3.32 \cdot 10^{-2}$ )		
$T_w$	$-3.23 \cdot 10^{-4***}$ ( $5.72 \cdot 10^{-5}$ )	$-3.36 \cdot 10^{-4***}$ ( $5.70 \cdot 10^{-5}$ )	$-3.68 \cdot 10^{-4***}$ ( $5.81 \cdot 10^{-5}$ )
$b$	$-5.75 \cdot 10^{-2***}$ ( $7.46 \cdot 10^{-3}$ )	$-6.14 \cdot 10^{-2***}$ ( $7.42 \cdot 10^{-3}$ )	$-1.02 \cdot 10^{-1***}$ ( $1.21 \cdot 10^{-2}$ )
$\lambda/k$		$6.28 \cdot 10^{-2***}$ ( $3.19 \cdot 10^{-3}$ )	
$\lambda_P \alpha_P$			$-1.31 \cdot 10^{-3}$ ( $2.19 \cdot 10^{-3}$ )
$\lambda_P \alpha_P : b$			$4.06 \cdot 10^{-3***}$ ( $1.03 \cdot 10^{-3}$ )
Observations	5,000	5,000	5,000
F Statistic	559***	753***	589***

*Note:* \* $p < 0.1$ ; \*\* $p < 0.05$ ; \*\*\* $p < 0.01$

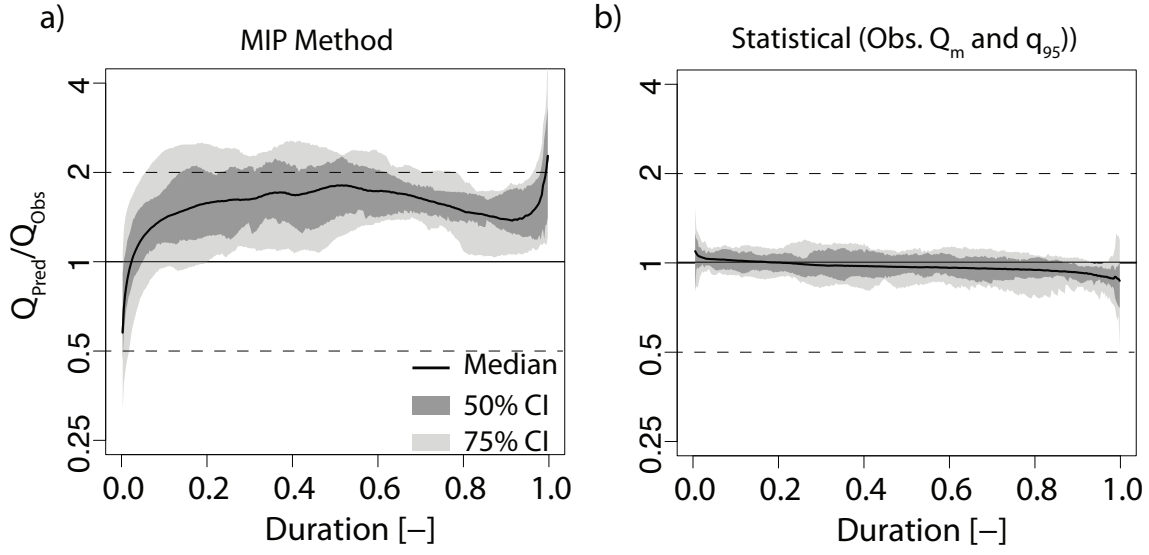


**Figure S1:** (a) Performance in ungauged basins of the MIP method currently used in Nepal for infrastructure design. The method produces significant upward biases on the predicted FDCs. (b) Error duration curve showing the prediction errors of the statistical methods when the parameters are estimated using observed streamflow, instead of linear regression. Comparison with Figure 2(b) of the main article shows that interpolation uncertainties on the model parameters are the main source of error of the statistical method.

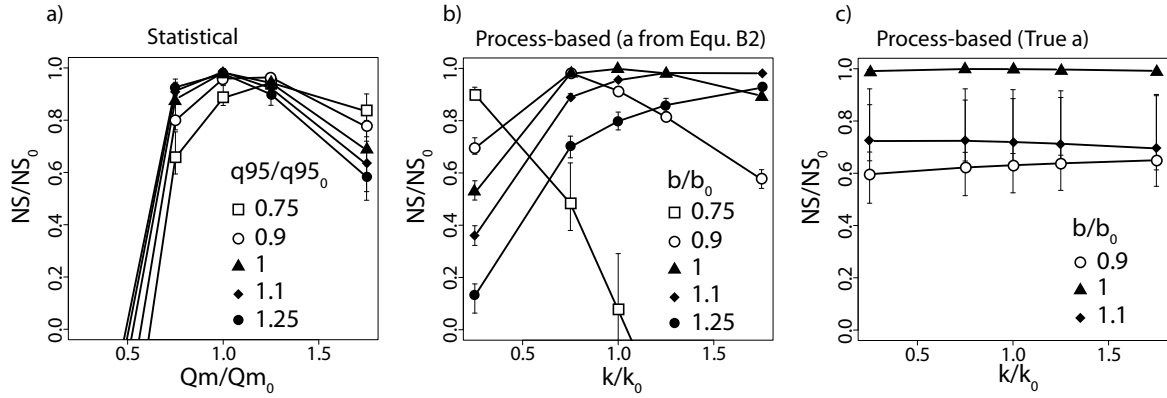


**Figure S2:** Effect of parameter estimation errors in the predictive performance of the models. Results were obtained using the Monte Carlo analysis described in Section S4, with errors in the parameters inserted instead of rainfall changes. (a) The performance of the statistical model is driven by errors in  $Q_m$ , with little effect of  $q_{95}$ . (b) The process-based model is sensitive to errors in both of its parameters, but  $k$  mostly affects prediction performance through its effect on  $a$  (Equation 2 of the main article). (c) Errors in  $k$  have little effect on modeling performance if the true values of  $a$  are used instead of Equation of the main article.

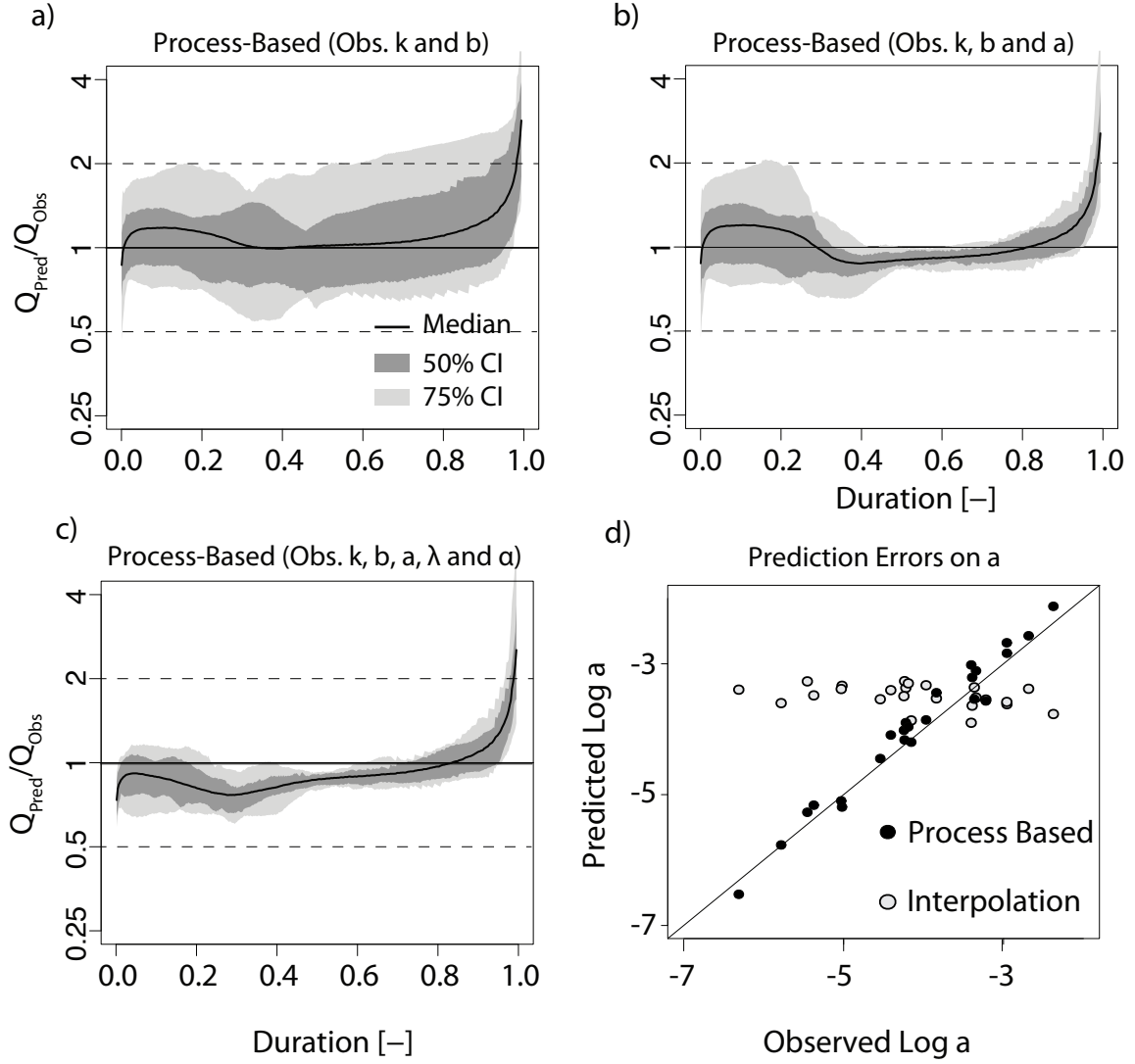


**Figure S3:** (a - c) Error duration curve of leave-one-out cross-validations for the process-based model using (a) observed values (i.e. estimated from local streamflow observations) for  $k$  and  $b$ , (b) observed values of  $k$ ,  $b$  and  $a$ , and (c) observed value of  $k$ ,  $b$ ,  $a$ ,  $\lambda$  and  $\alpha$ . Comparing panels (a) to (c) shows that errors in low flow decrease substantially when using observed values for  $a$ , instead of its approximation from  $k$  and  $b$  (Equation 2 in main article), whereas errors in high flow decrease substantially when using streamflow, instead of rainfall (see Appendix A of the main article), to estimate  $\lambda$  and  $\alpha$ . (d) Scatterplot of observed vs predicted values for  $a$ . Predictions errors are small when using Equation 2 of the main article with observed values of  $k$  and  $b$  (black), and significantly larger when interpolating  $a$  from observed values in neighboring catchments using ordinary kriging (grey).



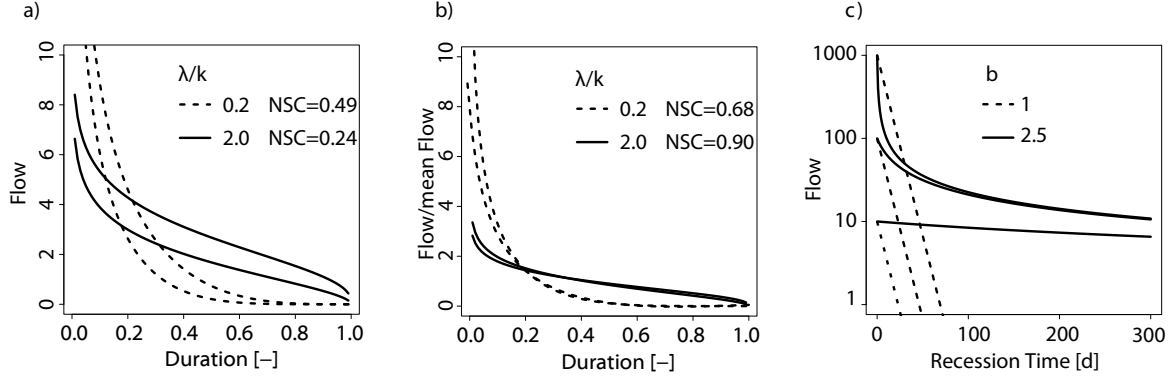


**Figure S4:** Streamflow resilience to rain changes. (a) Effect of a 50% increase of rainfall frequency on wet-season FDCs for different flow regimes. The solid FDCs assume a persistent regime ( $\lambda/k = 2.0$ ), with lower and upper curves representing the 'current' and 'future' flow distribution respectively. The dashed curves assume an intermittent regime ( $\lambda/k = 0.2$ ). The persistent regime (solid) is more sensitive to changes than the intermittent regime (dashed), as seen in its lower Nash Sutcliffe Coefficient (NSC) of 0.24. (b) The FDCs presented in panel (a) are normalized by their mean flow. The intermittent regime (dashed) is now more sensitive to change than the resilient regime (solid) because high flows are disproportionately affected by changes in rainfall. (c) Seasonal recession curves for linear (dashed) and non-linear (solid) catchments with different initial flow conditions. The figure illustrates that the shape of the recession is affected by initial conditions only if the catchment recessions are non-linear. For identical relative changes in initial conditions (here 1000%), the effect on recession shape is most important for low initial flow conditions.